

We get technical

Virtual antennas simplify IoT embedded antenna design

Quickly create low-jitter, high-frequency clocks using a translation loop module

How to select and apply antennas for IoT devices

Learn the fundamentals of software-defined radio



DigiKey



contents

- 4** Virtual antennas simplify IoT embedded antenna design
- 8** Quickly create low-jitter, high-frequency clocks using a translation loop module
- 14** How to implement SWaP-C satcom antenna arrays using SMD power dividers and directional couplers
- 20** Use an agile RF transceiver in an adaptive SDR communication system for aerospace and defense
- 26** Why a good LNA is key to a viable antenna front-end
- 30** **Special feature: retroelectro** Wildman Whitehouse and the twenty-five-hundred-mile-long capacitor
- 48** How to quickly leverage Bluetooth AoA and AoD for indoor logistics tracking
- 54** How to select and apply antennas for IoT devices
- 60** Learn the fundamentals of software-defined radio

Editor's note

Radio Frequency (RF) technology lies at the heart of modern communication, enabling the wireless systems that connect our devices, homes, and industries. From high-speed 5G networks and satellite communications to IoT devices and automotive radar systems, RF systems power the invisible networks shaping our world. For engineers, understanding RF design and its challenges is essential to pushing the boundaries of what's possible in electronics.

RF design is a unique and complex field, demanding a blend of theoretical knowledge, practical expertise, and creative problem-solving. Unlike digital systems, where signals are binary and predictable, RF operates in a dynamic analog domain, where even minor adjustments can have significant effects on performance. Engineers working with RF systems must consider factors like signal integrity, power management, and noise reduction while navigating real-world constraints such as size, cost, and regulatory compliance.

The growing demand for wireless technologies has raised the stakes for RF design, pushing engineers to innovate at unprecedented speeds. Whether it's ensuring the reliability of critical communications in aerospace systems or optimizing power efficiency for battery-operated IoT devices, RF design challenges are more diverse than ever. This diversity calls for a deep understanding of not just the theory but also the components, tools, and techniques that drive successful designs.

At DigiKey, we recognize the unique challenges engineers face in the RF domain. Designing high-performance systems requires access to the right components, tools, and resources, as well as a strong grasp of the principles that govern RF behavior. By bringing together innovative products and expert support, we aim to help engineers overcome these challenges and develop solutions that meet the demands of today's connected world.

This e-book is designed to inspire and support engineers tackling RF design projects. It is not just a guide to understanding RF technology but a resource for addressing the practical complexities of modern RF systems.





Virtual antennas simplify IoT embedded antenna design

Antennas have always existed in a contradictory and sometimes confusing place in the wireless world. On one side, they are just simple passive transducers between the confined energy in conductors as represented by voltage and current, and the dispersed, radiating electromagnetic energy existing in a vacuum or air. On the other side, they are available in a bewildering range of physical embodiments, configurations, styles, and sizes. Since the earliest days of wireless

(think Marconi and over a century ago), the conception, design, and fabrication of antennas has gone through several major phases.

The first phase

The first antennas were based on one of two fundamental structures: the monopole with an associated ground plane (sometimes called a whip antenna) (Figure 1), and the balanced, ungrounded dipole in various configurations such as the folded dipole (Figure 2). While

researchers and engineers knew that antenna performance was ultimately governed by Maxwell's four crisp equations, making use of these equations for antenna design was not possible due to the enormous complexities involved in modeling and computation.

As a result, antenna-related

Written by
Bill Schweber

analysis was limited to basic equations which were used to size the elements of antennas such as the monopole, dipole, long wire, and a few other configurations. These equations were also modified using rules of thumb, intuition, and field trials. For example, it was known that using tubing rather than thin wires for dipoles increased their bandwidth, which might be good or bad depending on the application; the amount of this increase versus tubing diameter was estimated using guidelines based on experience and basic measurements. Even academic discussions of antenna designs and their operating principles had few equations beyond basic arrangement versus wavelength discussions, as made clear in the 1926 technical paper for the classic Yagi-Uda antenna (Reference 1) (Figure 3).

The second phase

The second wave of antenna-design innovation began with

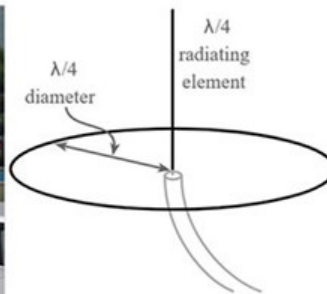


Figure 1: The long wire or whip antenna arrangement is a single-element design using a ground plane (here, the car's surface) (left); the illustration shows its simplicity (right). Image sources: Lihong Electronic (left); Electronics Notes (right)

the availability of models and algorithms that captured antenna attributes, which could be executed on computers to solve the electromagnetic field models and equations in a reasonable amount of time, as long as the models were not too complicated.

These “field solvers” allowed designers of new antenna configurations to use the combination of antenna theory and field-experience insight to propose new arrangements, model them, and finally quantify their performance “on paper”, without need for a physical model and field tests in their initial design stages. This approach worked to some extent, but it was still somewhat of a hit-or-miss arrangement. It did, however, enable engineers to focus on an antenna design and iteratively adjust and tweak it until it met the project objectives.

An extraordinary example of this was seen in the development of the first stealth aircraft, the F-117 Nighthawk, at Lockheed's

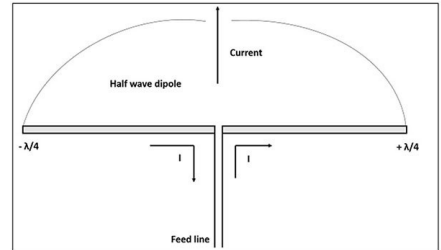


Figure 2: The basic dipole is a balanced, symmetrical antenna without a ground reference (top), as shown in the illustration (bottom). Image sources: TCARES.net (top) and Tutorials Point (bottom)

legendary Skunk Works (References 2 and 3). Much of the theoretical work on reducing its radar signature by many orders of magnitude was based on analytical solutions and complex equations.

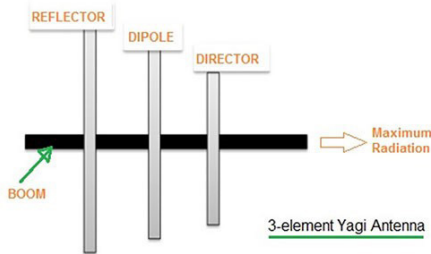
These equations analyzed the reflection of electromagnetic energy fields on the aircraft as it was bathed in radar signals. The project's objective was to use unique and unconventional choices in skin-panel material, shape, size, angles, joints, and other design elements to minimize the inherent tendency of these surfaces to act as an antenna. This, in turn, caused the aircraft to re-radiate and reflect energy in an antenna-like mode, and thus be invisible to the radar system receiver.

Third phase is very different

We are now entering a new wave of



Figure 3: The basic Yagi antenna (top) is a three-element antenna widely used in commercial, residential, and military applications. The three elements (bottom) are a driven (active) dipole element with a passive reflector behind it and a passive director in front of it, all mounted on a single boom. Image sources: EuroCaster/Denmark (top); RFWireless-World (bottom)



model-based antenna design, one which looks at the challenge from a different perspective. Instead of relying on a dedicated antenna to radiate an RF signal, the Internet of Things (IoT) device or smartphone radiates the signal directly from the ground plane.

To do this, a conventional embedded antenna is replaced with an Ignion NN03-320 DUO mXTEND antenna booster (Figure 3), a 7.0 millimeter (mm) long × 3.0 mm wide × 2.0 mm high passive component that is roughly one-tenth the size of a traditional antenna (note that Ignion was known as Fractus Antennas until 2021).

With its unique and patented Virtual Antenna technology – the commercial name for the “antenna-less” technology based on a new generation of tiny components – this booster is always the same component regardless of the size or form factor of the printed circuit

board. The designer tunes it to the desired frequency band(s) by creating and adjusting the matching network’s component arrangement and values.

In other words, this arrangement creates a new and beneficial synergy between the antenna booster and the surrounding ground plane. A rough analogy would be the effect of attaching a small audio-piezo driver to a rigid tabletop: the tabletop would resonate and, in effect, significantly boost the resultant audio output level.

The Ignion antenna boosters are standard, off-the-shelf, surface-mount components that replace conventional customized planar inverted-F antennas (PIFAs) and printed-circuit antennas. They are much smaller than the operating wavelength, typically below 1/30 or even 1/50 of the wavelength and beyond. They provide fully

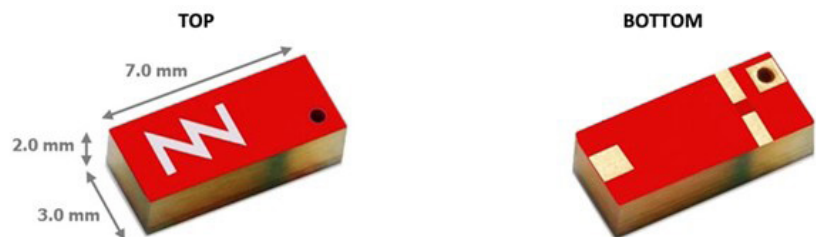


Figure 4: The Ignion NN03-320 DUO mXTEND is a tiny passive component that uses a product’s circuit board ground plane to radiate the RF signal. Image source: Ignion

functional multiband wireless connectivity, enabling a single antenna booster component to function effectively across multiple mobile and wireless designs, thus reducing time to market, product development investments, and of course, cost. In addition, as the antenna boosters are physically built as chip antennas, they can be installed using conventional pick-and-place systems, resulting in lower production cost and improved quality and reliability.

Making a match

The matching network is key to realizing the unique booster performance. While the antenna booster is standard and can be used across a variety of mobile products, the matching network does need customization for every product, but this is a one-time, up-front design effort.

By changing the matching network, the booster’s RF response can be customized to cover the multiple frequency bands required in a modern IoT device or smartphone. The simpler single-band IoT device needs a matching network with typically three to five

| Class | Frequency Regions | Frequency Range | More detailed info |
|---------|-------------------|--|--------------------|
| 2 Ports | 4 | 1561MHz, 1575MHz, 1598MHz to 1606MHz, and 2400MHz to 2500MHz | GNSS + BLUETOOTH |
| 1 Port | 3 | 1561MHz, 1575MHz, 1598MHz to 1606MHz | GNSS |
| 1 Port | 1 | 2400MHz to 2500MHz | BLUETOOTH |
| 1 Port | 1 | 3400MHz to 3800MHz | 5G |
| 1 Port | 1 | 3100MHz to 4800MHz and 6000MHz to 10600MHz | UWB |

components, while a multiband smartphone might need a couple of boosters and five to eight high-Q components for its matching network.

Ignion simplifies the design effort with a free development tool which lets the designer virtually place the booster near the edge of the circuit board, define a “clear” zone around the booster devoid of components, and then calculate the needed passive components for the matching network. For the multiport NN03-320, the calculated matching networks allow the device to cover multiple bands and applications including GNSS, Bluetooth, 5G and UWB, over frequencies spanning 1561 to 1606 megahertz (MHz), 2400 to 2500 MHz, 3400 to 3800 MHz, 3100 to 4800 MHz, and 6 to 10.6 gigahertz (GHz) (Figure 5).

The NN03-320 datasheet specifies the performance of this 50 ohm (Ω) Virtual Antenna booster component and optimized matching network using standard antenna parameters for each band, including efficiency,

peak gain, VSWR, polarization, and radiation pattern.

Application notes show typical matching network schematic diagrams like Figure 6, and include a table of suggested passive component values for each desired frequency span. While these values serve as starting points, they will need to be tweaked to account for unanticipated parasitics, as well as the effects of nearby components such as displays or ICs.

Conclusion

Antenna boosters such as these from Ignion represent a different way of radiating RF energy by using

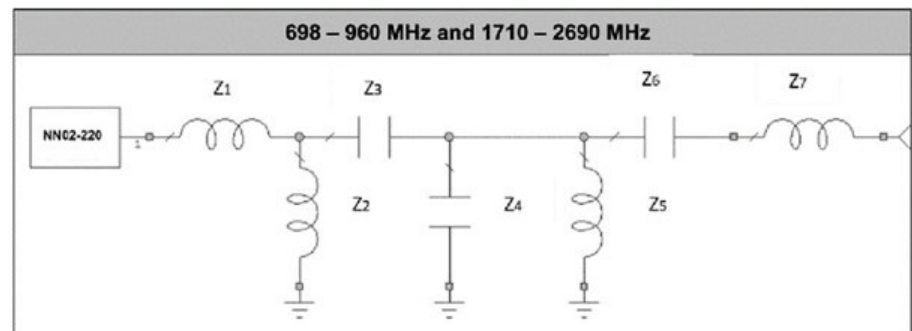


Figure 6: This suggested schematic diagram for a dual-band matching network also comes with a table of suggested passive component values to provide a starting point for design, analysis, and evaluation. Image source: Ignion

Figure 5: The NN03-320 antenna booster can be used for different and/or multiple bands when fitted with the suitable passive component matching circuit between the RF source and the booster. Image source: Ignion

the ground plane as a radiating surface. These passive, surface-mount booster devices offer an alternative to conventional embedded antenna arrangements for IoT devices and smartphones. A single Virtual Antenna device can serve different parts of the RF spectrum, simply by appropriate configuration of its passive matching network.

Recommended Reading

1. Yagi, Hidetsu; Uda, Shintaro, Proceedings of the Imperial Academy (February 1926). [“Projector of the Sharpest Beam of Electric Waves”](#) (PDF).
2. Air Force Magazine, [“How the Skunk Works Fielded Stealth”](#)
3. Ben Rich, [“Skunk Works: A Personal Memoir of My Years of Lockheed”](#)

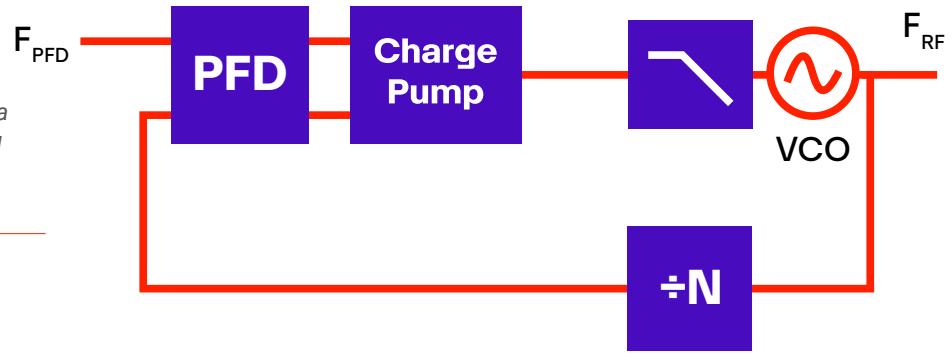
Quickly create low-jitter, high-frequency clocks using a translation loop module

Written by Bonnie Baker





Figure 1: The standard PLL locks to a lower frequency (F_{PFD}) reference and generates an output frequency (F_{RF}).
Image source: Bonnie Baker



Designers of instrumentation and measurement systems require low-jitter, spurious-free signals in order to provide the signal-to-noise ratios (SNRs) or error vector magnitudes (EVMs) required to meet increasingly demanding customer requirements. At the same time, they are also facing significant pressure to reduce board footprint as well as design cost, and complexity. The latter is critical in to shortening development time to meet narrowing time-to-market windows.

To address the many application challenges, engineers need to transition their instrumentation and measurement clocking solutions from custom-made traditionally discrete designs to more integrated solutions. An important step toward this is to use an integrated translational phase-locked loop (PLL). This allows the frequency up-conversion of a traditional voltage-controlled oscillator (VCO) signal, while substantially maintaining the jitter and phase noise of a fixed external local oscillator (LO).

This article discusses the role of

translation loops towards achieving the industry lowest integrated phase noise. By way of example, it introduces the [ADF4401A](#) translation loop system-in-package (TL SiP) from [Analog Devices](#) and shows how it addresses performance requirements through an output signal with sub-10 femtosecond (fs) rms wideband integrated jitter capability and enhanced isolation to attenuate spurious components, while also meeting designers' integration, cost, complexity, and time-to-market needs.

Traditional PLL vs. translation loop operations

The primary purpose of a translation loop is to generate an output signal locked to an input reference signal with significantly reduced in-band phase noise compared to traditional PLLs.

A standard PLL consists of a feedback system containing a phase-frequency detector (PFD), charge pump, low-pass filter (LPF), VCO, and a feedback frequency

divider N (Figure 1).

The PFD compares the phase of input reference and the phase of the feedback signal and generates a series of pulses proportional to the phase error between them. The charge pump receives the PFD pulses and converts them into current source or sink pulses that will in turn tune the VCO either up or down in frequency. The LPF removes all the pulses' high-frequency energy and converts them into a voltage that the VCO can use. The VCO's output signal is fed back to the PFD block through the N divider to complete the loop.

Figure 1's frequency transfer function is calculated using Equation 1:

$$F_{RF} = X \times F_{PFD}$$

Where F_{RF} is the output frequency
N is the feedback divider ratio (can

Figure 2: For a standard PLL in this example, the noise from the feedback divider ($20 \log_{10}(N)$) has a 34 dB higher in-band noise compared to the lower yellow plot where $N = 1$. Image source: Bonnie Baker

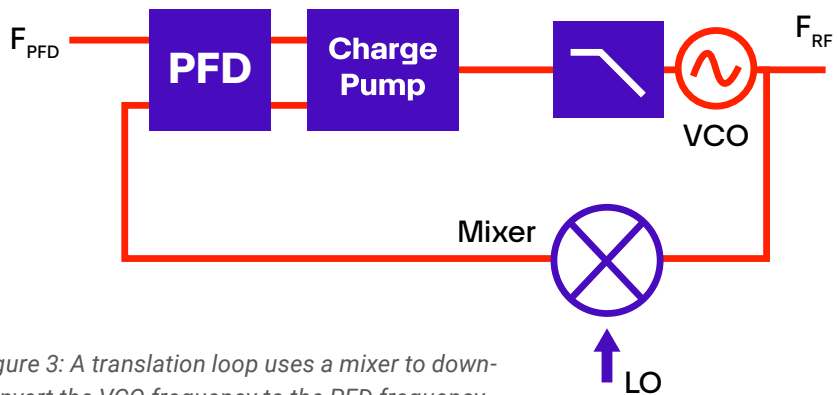
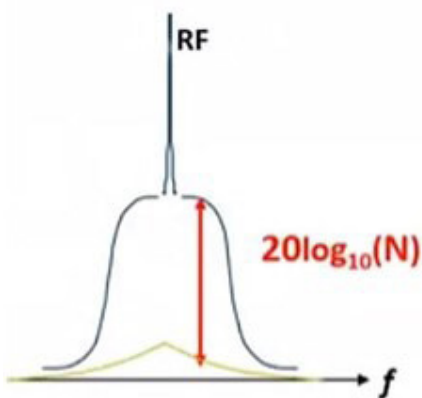


Figure 3: A translation loop uses a mixer to down-convert the VCO frequency to the PFD frequency instead of using a traditional feedback divider.

Image source: Bonnie Baker

be integer or fractional)

F_{PFD} is the PFD frequency

Figure 1's in-band noise floor is calculated using Equation 2:

$$\text{In-band noise floor} = FOM_{PLL} + 10 \log_{10}(F_{PFD}) + 20 \log_{10}(N)$$

Where FOM_{PLL} is the PLL's in-band phase noise floor figure of merit (FOM)

Consider an example with an in-band phase noise floor FOM of -234 decibels per Hertz (dB/Hz); a PFD frequency (F_{PFD}) of 160 megahertz (MHz), and an output frequency (F_{RF}) of 8 gigahertz (GHz).

For this system, Equation 1 is used to calculate the value of N:

$$F_{RF} = N \times F_{PFD}$$

With the translation loop architecture, the phase noise of the Offset LO is very important to achieve the best performance at the RF output

$$8,000 \text{ MHz} = N \times 160 \text{ MHz}$$

$$N = 50$$

Equation 2 is used to calculate the in-band noise floor:

$$\begin{aligned} \text{In-band noise floor} &= FOM_{PLL} + 10 \log_{10}(F_{PFD}) + 20 \log_{10}(N) \\ &= -234 \text{ dBc/Hz} + 10 \log_{10}(160 \text{e}6 \text{ Hz}) \\ &\quad + 20 \log_{10}(50) \\ &= -118 \text{ dBc/Hz} \end{aligned}$$

In the calculation above, the N divider strongly contributes to the overall in-band noise floor, with $20 \log_{10}(50)$, equaling 34 dB. A smaller N value would decrease the in-band noise floor; however, it would also decrease the output frequency. So how do we generate a high output frequency and keep a lower loop gain (N)?

The solution to this issue is to replace the N-divider with a down-converting mixing stage (Figure 3).

In Figure 3, the mixer replaces the feedback N divider, resulting in a loop gain equal to 1 (N=1). This operation will greatly diminish the contribution of the feedback loop to the in-band noise floor. For the in-band noise calculation, the value of N is now equal to 1. Using Equation 2, the in-band noise floor for the modified system is as follows:

$$\begin{aligned}
 \text{In-band noise floor} &= \text{FOM}_{\text{PLL}} + 10 \log_{10}(\text{F}_{\text{PFD}}) + 20 \log_{10}(N) \\
 &= -234 \text{ dBc/Hz} + 10 \log_{10}(160\text{e}6 \text{ Hz}) + 20 \log_{10}(1) \\
 &= -152 \text{ dBc/Hz}
 \end{aligned}$$

The new in-band noise shows an improvement of 34 dBc/Hz.

In Figure 3, the mixer depends on an extremely low noise LO, called Offset LO. $F_{\text{LO}} \pm F_{\text{RF}}$ must equal F_{PFD} to achieve lock.

With the translation loop architecture, the phase noise of the Offset LO is very important to achieve the best performance at the RF output. For this reason, engineers would typically design an Offset LO based on voltage-controlled surface acoustic wave (SAW), or oscillators (VCSOs), or comb generators, or dielectric resonator oscillators (DROs). NOTE: For support with designing an Offset LO, contact Analog Devices.

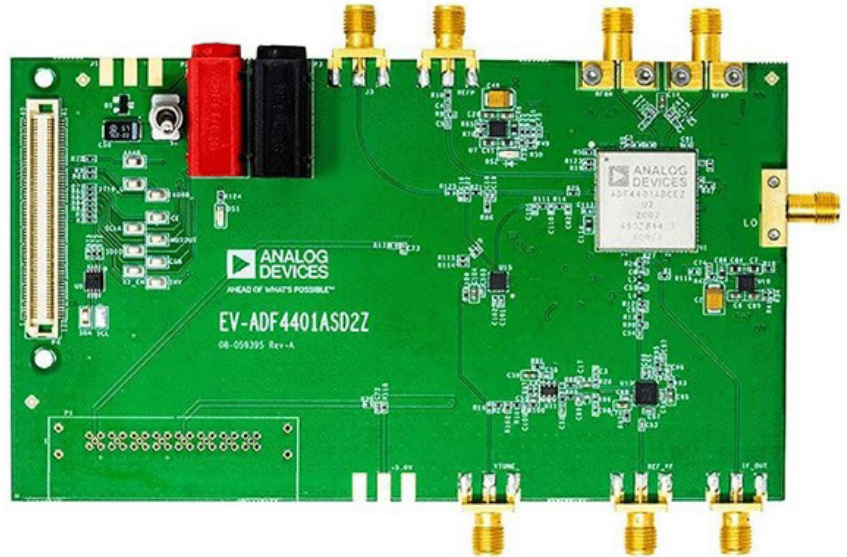


Figure 4: The EV-ADF4401ASD2Z evaluation board for the ADF4401A translation loop module includes an external PFD, a USB interface, and voltage regulators. Image source: Analog Devices

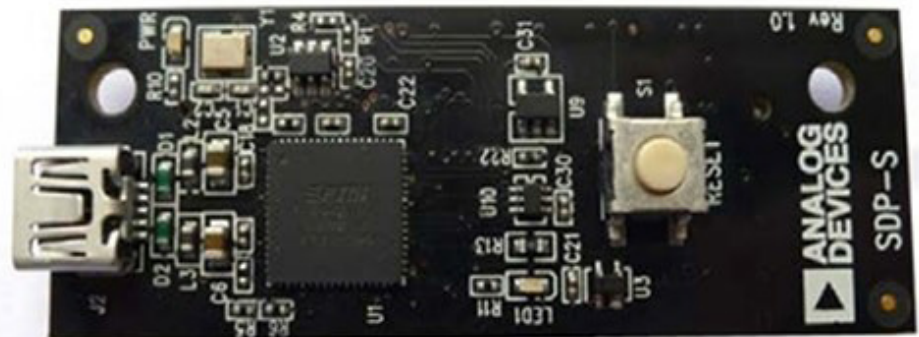
Translation loop challenges

Traditionally, the design of a low-noise translation loop involves the implementation of numerous circuit blocks, resulting in a complex design, usually large, and with limited flexibility. In addition, the entire circuit must be validated and characterized for the target operation. For example, one major design concern is LO leakage (LO to RF isolation) to the RF

output signal. This is a significant challenge for engineers to address. With traditional designs, engineers usually proceed to multiple design iterations to achieve optimized performance and suitable isolation.

Figure 3 shows how the ADF4401A integrates major circuit blocks to provide a fully characterized solution and eliminates the traditionally difficult areas related to the performance and isolation

Figure 5: The EVAL-SDP-CS1Z (or SDP-S) controller board is required to provide a USB connection from the EV-ADF4401ASD2Z to a PC for programming. Image source: Analog Devices



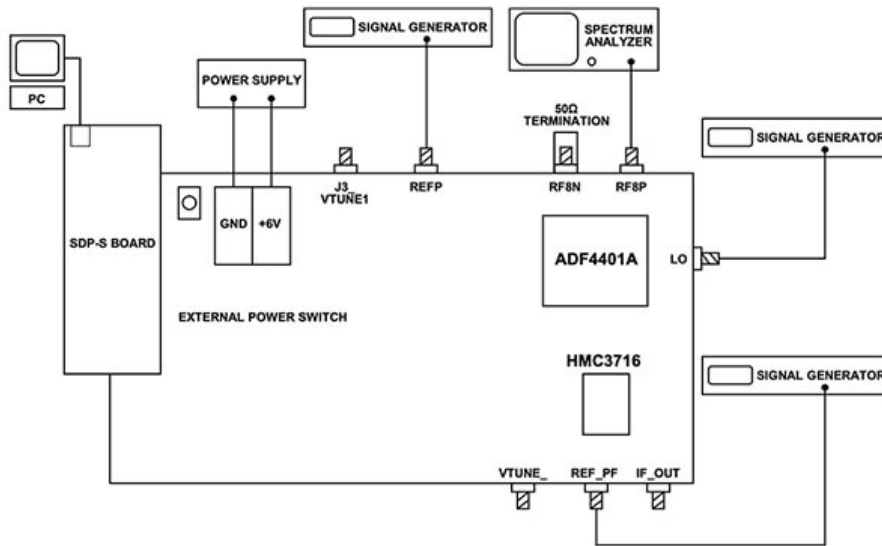


Figure 6: An EV-ADF4401ASD2Z setup diagram shows the equipment and connections required to evaluate the ADF4401A, including the SDP-S control board, PC, power supply, signal generators, and spectrum analyzer.

Image source: Analog Devices

in translation loop designs. This programmable solution allows engineers to achieve optimized performance on the first effort and reduce time to market.

Evaluating the ADF4401A

The ADF4401A is designed to help engineers reduce the time to market of high-performance instrumentation, using a frequency generation solution with an RF bandwidth of 62.5 MHz to 8 GHz. By using a down-converting mixer, the ADF4401A has very low in-band noise with a wideband jitter of ~9 femtoseconds (fs) integrated from 100 Hz to 100 MHz. The design and layout techniques inside the ADF4401A enable a typical spurious-free dynamic range of 90 dBc. A package size of 18 x 18 x 2.018 millimeters (mm) substantially reduces board space

compared to a traditional discrete design.

To evaluate the device's performance, designers can use the [EV-ADF4401ASD2Z](#) evaluation board (Figure 4). The board includes a complete translation loop, including an external PFD (HMC3716), an active filter (LT6200), and a multiplexer (ADG1609).

The EV-ADF4401ASD2Z includes the ADF4401A TL SiP with integrated VCO, a loop filter (5 MHz), a PFD, a USB interface, and voltage regulators. Additionally, the EV-ADF4401ASD2Z requires the [EVAL-SDP-CS1Z](#) (SDP-S) system demonstration platform (SDP) (serial) controller board (Figure 5). The board provides a USB connection from a PC to the EV-ADF4401ASD2Z so it can be programmed. The controller

board is not provided in the EV-ADF4401ASD2Z kit.

Figure 6 maps out the physical connections of the EV-ADF4401ASD2Z system. The associated [Analysis | Control | Evaluation \(ACE\)](#) Software controls the TL SiP functions. Power is derived from an externally applied 6-volt power supply.

The suggested equipment to use with this evaluation board includes a Windows PC, a spectrum analyzer or a signal source analyzer, and three signal generators.

The block diagram of the EV-ADF4401ASD2Z shows the ADF4401A module, along with Analog Devices' [HMC3716](#) PFD, [LT6200](#) op-amp, and the [ADG1219](#) SPDT switch (Figure 7).

It is vital to use a PFD that can operate at high frequencies as this minimizes the need for dividers, which can degrade the in-band noise response. The 1.3 GHz phase comparison frequency capability of Analog Devices' HMC3716 makes it ideal for use in the IF range of the ADF4401A. The ability of such a circuit to compare both frequency and phase eliminates the need for additional circuitry to steer the frequency to the intended output frequency. The HMC3716 becomes the external PFD to complete the offset loop. The high-frequency operation range and ultra-low phase noise floor of the HMC3716 make it possible to design wide-bandwidth loop filters.

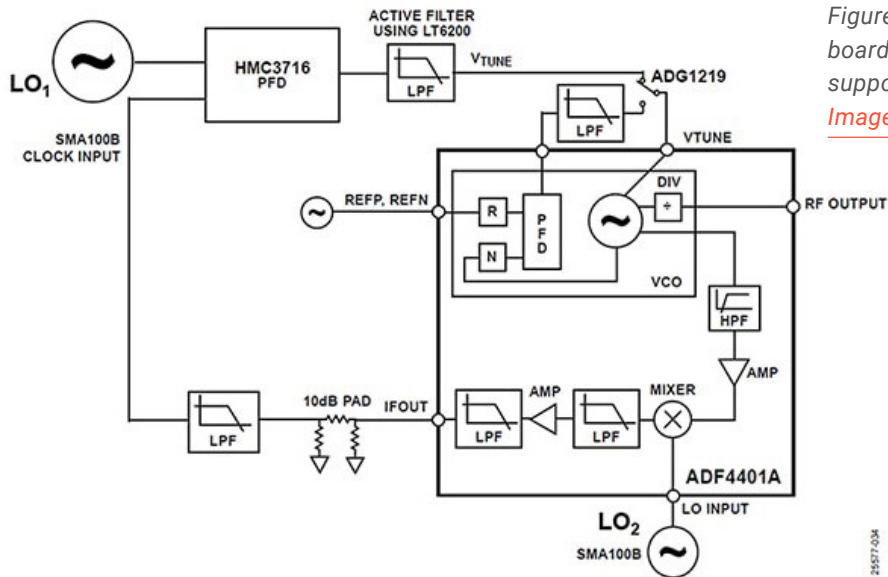


Figure 7: The EV-ADF4401ASD2Z evaluation board block diagram shows the key components supporting the AD4401A translation loop. Image source: Analog Devices

In Figure 7, the LT6200 op-amp with an LPF configuration attenuates high-frequency spurs, while the ADG1219 switch completes the system's translation loop.

The EV-ADF4401ASD2Z evaluation fixture creates in-band noise plots and jitter measurements as shown in Figure 8.

In Figure 8, the LO2 and HMC3716

input is an SMA100B RF and microwave signal generator. The evaluation board's LO2 in-band noise is approximately -135 dBc/Hz which is apparent at low offsets up to 300 kHz. The LO2, ADF4401A module, HMC3716 PFD, and loop filter contribute to an in-band noise of about -140 dBc/Hz. The internal phase noise appears between 5 MHz and 50 MHz, and the

phase noise floor of the fixture is approximately -160 dBc/Hz. These together give an rms jitter of 12.53 fs in total.

Conclusion

High-speed instrumentation systems require extremely low-jitter clocks to ensure that the output data remains uncompromised. The challenge for engineers is to find suitable devices that can build the high-speed gigahertz clock system. The ADF4401A translation loop greatly simplifies device selection to build the clock system, providing a compact module that ensures low jitter at higher frequencies, while also reducing board space, cost, and time to market.

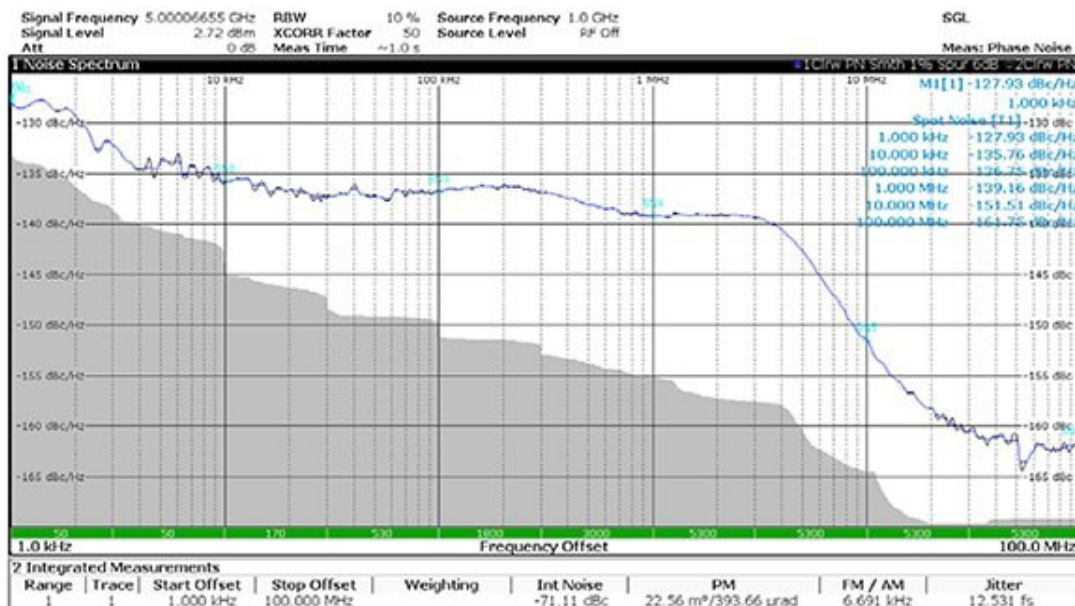


Figure 8: Single sideband phase noise at 5 GHz output, with an external HMC3716 reference of 500 MHz and external LO at 4.5 GHz. Image source: Analog Devices

How to implement SWaP-C satcom antenna arrays using SMD power dividers and directional couplers

Written by Steven Keeping

The space around the Earth is filling fast, and thousands more new satellites are due for launch in the next decade. That's putting pressure on satellite communications (satcoms) designers from two sides. First, available bandwidth for satcoms in the traditional L, C and X bands is fast being used up. Secondly, commercial satellite builders want their products to be lighter and cheaper to launch.

Satcom designers are responding to the lack of RF bandwidth by moving communications from the traditional satellite bands to higher frequency RF bands such as Ku (12 to 18 gigahertz (GHz)). The Ku band offers the potential for greater throughput and is much less congested. With respect to the demand for minimal size, weight, power, and cost ("SWaP-C"), designers are responding by building key elements of the

satellite, such as the antenna array, using advanced packaged surface mount devices (SMDs).

This article outlines the benefits of SMD power dividers and directional couplers, key passive elements used in Ku band satcom antenna arrays. The article introduces example devices from Knowles Dielectric Labs, describes how these components meet today's low-SWaP demands, and how designers can use key performance characteristics of these vital components to optimize antenna array performance.

Advances in antenna arrays

Recent developments in satellite and ground station antennas have seen a move away from single-antenna dishes to antenna arrays. Antenna arrays combine two or more elements, each of

which essentially perform as mini antenna. The benefits of antenna arrays compared to a conventional antenna for satcoms applications include:

- Higher gain
- Increased signal-to-noise ratio (SNR)
- Steerable transmission beams and enhanced sensitivity to incoming signals from a particular direction
- Better diversity reception (helps overcome signal fading)
- Smaller side lobes in the antenna radiation pattern

The conventional array structure comprises a 3D-brick configuration made up of electronic assemblies placed side-by-side and attached using multiple connectors and cables. This increases the bulk and complexity of an antenna array, compared with single-antenna dishes.



The solution to this bulk and complexity has come from a focus on low SWaP-C that eliminates the brick-like structure resulting from chip-and-wire or hybrid fabrication techniques. Newer designs are made up of multiple microstrip 2D planar elements based on a pc board substrate using SMD packaging. This planar configuration removes the need for many connectors and cables, enhancing SWaP while increasing reliability and simplifying manufacturing (Figure 1).

SMDs not only considerably reduce the bulk of the antenna array, but they also allow for the use of a single automated assembly line, dramatically reducing the cost of production compared to a conventional chip-and-wire or hybrid approach. SMD assembly also helps accelerate time to market.

Such advances have been made possible because of a new generation of SMD components that can perform reliably in space at high operational frequencies. The devices feature innovative dielectrics, tight tolerance, thin-film manufacturing, and novel microstrip line topologies to

Figure 1: The use of low SWaP-C SMD components (right) allows for a reduction in the bulk of satcom antenna arrays compared with a conventional 3D brick assembly (left). Image source: Knowles DLI

provide a high performance/footprint ratio.

Key antenna array components: power divider

A critical passive SMD in the antenna array is the power divider. Individual power dividers split an incoming signal into two or more signals to distribute across the antenna elements making up the array. In its simplest form, the power divider splits the input power (minus some circuit losses) evenly across each output leg, but other forms of power dividers enable the input power to be proportionally shared across the output legs.

There are several power divider configurations, but for high-frequency applications, power dividers typically take the form of a microstrip line Wilkinson design (Figure 2). In the basic form, each

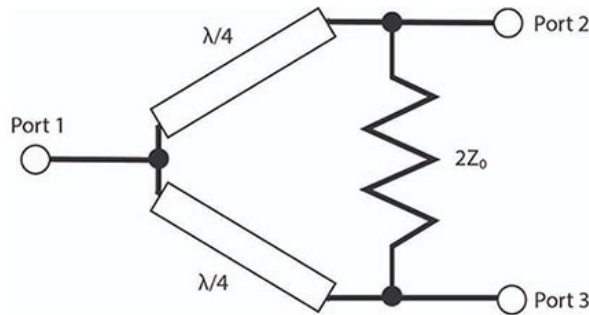


Figure 2: The basic Wilkinson power divider uses two quarter wavelength impedance transformers and an isolating resistor to match the output ports. Ports 2 and 3 each deliver half the Port 1 input power. Image source: Knowles DLI

leg of the divider measures one quarter the wavelength of the incoming RF signal. For example, for an incoming signal with a center frequency of 15 GHz, each leg would be 5 millimeters (mm) in length. The legs operate as quarter-wavelength impedance transformers.

An isolating resistor is used to match the output ports; because there is zero potential between the output ports, no current flows through the resistor so it doesn't contribute to resistive losses. The resistor also provides excellent isolation, even when the device is used in reverse (as a power combiner), thereby limiting crosstalk between individual channels.

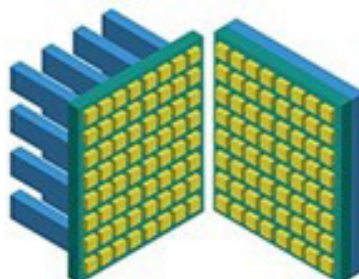
To limit losses as the power is being split, the two output ports of the power divider must each appear as an impedance of $2 Z_0$. (The $2 Z_0$ in parallel will present an overall impedance of Z_0 .)

For an equal power distribution with $R = 2 Z_0$, then:

$$Z_{match} = \sqrt{2} Z_0 = 1.414 Z_0$$

Where:

R = the value of the terminating resistor connected between the



two ports

Z_o = the characteristic impedance of the overall system

Z_{match} = the impedance of the quarter wave transformers in the legs of the power divider

A scattering matrix (S matrix) contains the scattering parameters used to describe the electrical performance of an RF linear network such as a Wilkinson power divider. Figure 3 shows the S matrix for the simple form of power divider shown in Figure 2.

Key characteristics of the S matrix include the following:

- $S_{ij} = S_{ji}$ (showing the Wilkinson power divider can also be used as a combiner)
- The terminals are matched ($S_{11}, S_{22}, S_{33} = 0$)
- The output terminals are isolated ($S_{23}, S_{32} = 0$)
- The power is equally split ($S_{21} = S_{31}$)

Losses are minimized when the signals at Ports 2 and 3 are in phase and have equal magnitude. An ideal Wilkinson power divider delivers $S_{21} = S_{31} = 20 \log_{10}(1/\sqrt{2}) = (-3)$ decibels (dB) (i.e., half the input power at each output port).

Microstrip line Wilkinson power

$$[S] = -j/\sqrt{2} \begin{bmatrix} 0 & 1 & 1 \\ 1 & 0 & 0 \\ 1 & 0 & 0 \end{bmatrix}$$

Figure 3: Scattering matrix (S matrix) for the Wilkinson power divider shown in Figure 2. Image source: Steven Keeping

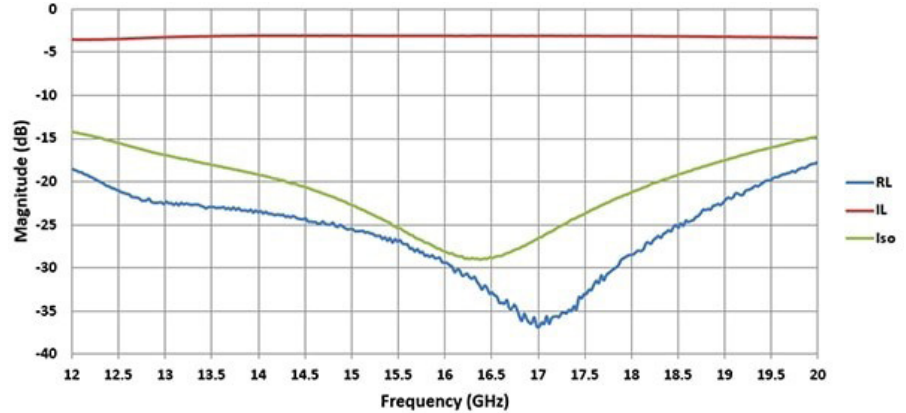


Figure 4: The PDW06401's power divider frequency response. RL represents terminal matching (S_{11}, S_{22} etc.), Iso is the isolation between output ports (S_{23}, S_{32}) and IL is the output power (S_{21}, S_{31}). Image source: Knowles DLI

dividers are a good solution for low SWaP-C antenna array applications. Commercial options for the Ku band include Knowles Dielectric Labs' PDW06401 16 GHz two-way Wilkinson power divider. Knowles dielectric and thin-film manufacturing know-how have allowed it to fabricate a low-loss, yet compact SMD for service with Ku band satcom antenna arrays.

The PDW06401 measures 3 x 3 x 0.4 mm and uses low-loss materials that minimize performance variation over a wide temperature range. The package's characteristic impedance (Z_o) matches the 50-ohm (Ω) requirement needed to minimize the voltage standing wave ratio (VSWR), and hence return losses in high-frequency RF systems. The device features zero nominal phase shift, an amplitude balance of ± 0.25 dB and a phase balance of $\pm 5^\circ$. Excess insertion losses are 0.5 dB. Figure 4 illustrates the PDW06401 power divider's frequency response.

The return loss, isolation, amplitude balance, and phase balance characteristics of a power divider are critical to the performance of the antenna array in the following ways:

- The return loss of the product should be low because greater losses directly compromise maximum transmitted or received beam energy
- Product isolation should be high because this impacts the isolation between signal paths in the antenna array and enhances its gain
- The device's amplitude balance should approach 0 dB as it affects the amplitude performance and Effective Isotropic Radiated Power (EIRP) of the antenna
- The device's phase balance should approach 0° difference as this promotes maximum power transfer and ensures intended phase length for all branches across the network. A large phase imbalance will deteriorate

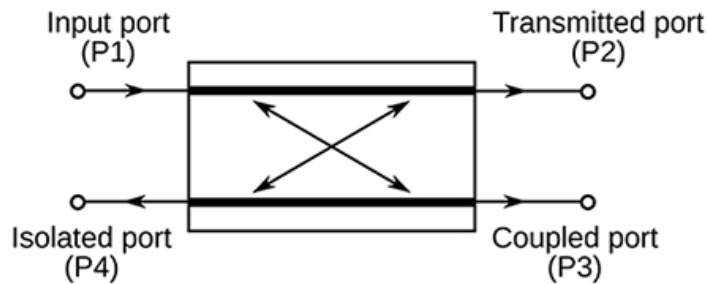


Figure 5: The coupled port (P3) of a power divider passes on some fraction of the power delivered to the input port (P1), with the rest passing through the transmitted port (P2). The isolated port (P4) is terminated with an internal or external matched load. *Image source: Spinningspark at Wikipedia*

EIRP and potentially change the radiation pattern of a beam-forming antenna array

Key antenna array components: directional coupler

The directional coupler is another component that performs an important role in antenna arrays by consistently measuring the transmit and receive power of the array elements. The directional coupler is a passive device which couples a known amount of transmission or receive power through to another port from where it can be measured. The coupling is typically achieved by positioning two conductors close to each other such that the energy passing through one line is coupled to the other.

The device has four ports: input, transmitted, coupled and isolated. The main transmission line is situated between Ports 1 and 2. The isolated port is terminated with an internal or external matched load (typically 50 Ω), while the coupled port (3) is used to tap the coupled energy. The coupled port

typically delivers a fraction of the energy of the main line and often features a smaller connector to distinguish it from the main line Ports 1 and 2. The coupled signal can be used to obtain signal power level and frequency information without interrupting the main power flow in the system. Power entering the transmitted port flows to the isolated port and does not affect the output of the coupled port (Figure 5).

The key characteristic of a coupler is the coupling factor.

This is defined as:

$$C_{3,1} = 10 \log (P_3/P_1) \text{ dB}$$

The simplest form of coupler features a right-angled topology whereby the coupled lines run adjacent for one quarter of the wavelength of the input signal (e.g., 5 mm for a 15 GHz signal). This type of coupler typically produces half the input power at Port 3 (i.e., it has a coupling factor of 3 dB), with the power at the transmitted port also reduced by 3 dB. (Figure 6).

As is the case with the power divider, there are some key characteristics of the directional coupler that impact the

performance of the antenna array.

These characteristics include the following:

- The main line loss should be minimized to enhance antenna array gain. This loss is due to resistive heating of the main line and is separate to the coupling loss. The total main line loss is the combination of resistive heating loss plus coupling loss
- The coupling loss is the reduction in power due to the energy transferred to the coupled and isolated ports. Assuming a reasonable directivity, the power transferred unintentionally to the isolated port should be negligible compared to that transferred intentionally to the coupled port
- The return loss should be minimized. This is a measure of the amount of the signal that

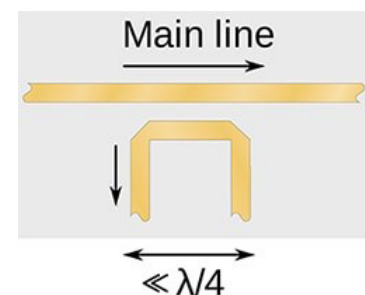


Figure 6: The simplest form of directional coupler features coupling lines running adjacent for a quarter wavelength of the input signal frequency. *Image source: Spinningspark at Wikipedia*

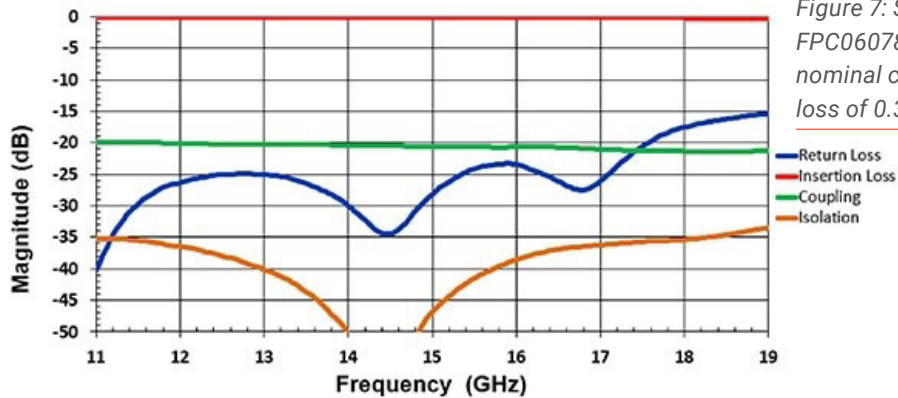


Figure 7: Shown is the frequency response of the FPC06078 directional coupler. The device exhibits a nominal coupling factor of -20 dB and a low insertion loss of 0.3 dB. Image source: Knowles DLI

range of 12 to 18 GHz. The FPC06078 directional coupler features an insertion loss of 0.3 dB and a minimum return loss of 15 dB. The device's directivity is 14 dB (Figure 8).

- is returned or reflected by the directional coupler
- The insertion loss should also be minimized. This is the ratio of a signal level in a test configuration without the directional coupler present, compared to that when the component is present
- Isolation should be maximized. This is the power level difference between the input port and the isolated port
- The directivity should be maximized. This is the power level difference between Port 3 and Port 4 of the directional coupler and is related to isolation. It is a measure of the independence of the coupled and isolated ports

While RF directional couplers can be implemented using a variety of techniques, it is the microstrip line type that are finding favor in low SWaP-C satcom applications because of their small size. One example is Knowles' [FPC06078](#) directional coupler. The device is an SMD microstrip line device that measures 2.5 x 2.0 x 0.4 mm. It has an operating temperature range of -55°C to +125°C and a characteristic impedance of 50 Ω.

While the coupling factor is frequency dependent, a high-quality directional coupler will exhibit a relatively flat coupling frequency response. From Figure 7 above, it can be seen that the Knowles

device exhibits a nominal coupling factor of 20 dB, which varies by only 2 dB across an operational

Conclusion

Designers are responding to the demand for low SWaP-C in satcom applications by employing compact SMD passive components. Examples include the power dividers and directional couplers used in the fabrication of the satellite's antenna arrays.

By selecting good quality compact SMD passive devices – that promise superior performance through microstrip line construction and ceramic materials with high dielectric capabilities – designers can take advantage of higher frequency RF bands for satcom applications. Moreover, this new generation of SMD power dividers and directional couplers enables designers to come up with smaller and lighter antenna arrays, while simultaneously enhancing the antennas' gain and beam forming capabilities.

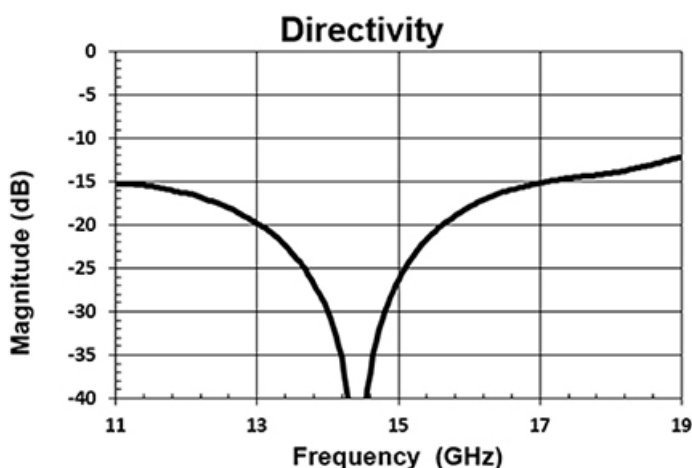


Figure 8: Shown is a graph of the FPC06078 directional coupler's directivity. For higher antenna array performance, the directivity, which is related to isolation, should be maximized. Image source: Knowles DLI

Use an agile RF transceiver in an adaptive SDR communication system for aerospace and defense

Written by Stephen Evanczuk





Figure 1: Traditional superheterodyne radio architectures can meet performance targets, but their complexity prevents them from meeting emerging targets for minimal SWaP. [Image source: Analog Devices](#)

Aerospace and defense (ADEF) system designers face unrelenting demand for lower power and more compact communications systems that are capable of an agile response to a dynamic signals environment. Moving beyond traditional radio architectures, software-defined radio (SDR) technology can help meet the fast-changing requirements for ADEF radios, but SDR implementation has presented multiple challenges for meeting both the functional requirements and the need for reduced size, weight, and power (SWaP).

This article describes a more effective SDR solution from [Analog Devices](#) that can simplify the design of low-power, compact, and agile communications systems without compromising performance.

Emerging challenges drive more demanding requirements

Designers face a demand for more effective communications in a growing number of industrial and mission-critical applications, including secure

radio communications, adaptive radar, electronic warfare, and enhanced GPS navigation. These new challenges drive a need for enhanced wideband operation, higher dynamic range, greater frequency agility, and reconfigurability. However, these more demanding functional requirements can conflict with the need for lower SWaP as communications systems move to smaller battery-powered platforms, including unmanned aerial vehicles (UAS) and portable units.

Design solutions based on traditional discrete superheterodyne radio architectures offer high performance, wide dynamic range, and minimal spurious noise. For designers, the challenge of isolating the desired signal from the intermediate frequency (IF) at the heart of this approach typically results in complex designs with high SWaP and little to no reconfigurability (Figure 1).

In contrast, direct conversion (zero-IF) architectures reduce both the filtering requirements and the need for very high-bandwidth analog-to-digital converters (ADCs), resulting in a simpler design that can be

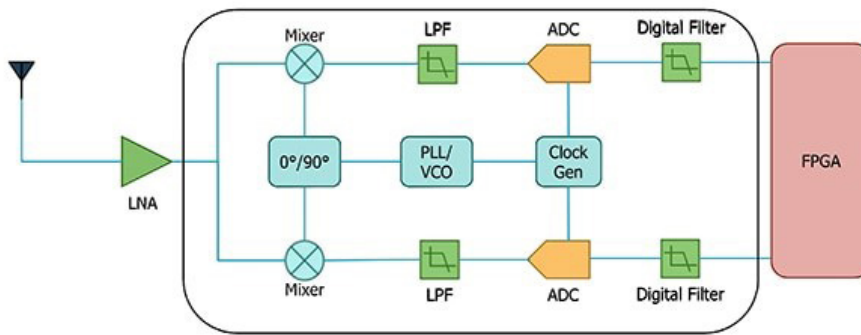


Figure 2: Zero-IF radio architectures can meet the need for higher performance and lower SWaP, but signal isolation is challenging. Image source: Analog Devices

implemented on a single chip (Figure 2).

Despite its apparent advantages, the direct conversion architecture presents its own implementation challenges that have limited its widespread adoption. In this architecture, the signal is converted to a radio frequency (RF) carrier at the local oscillator (LO) frequency, but direct current (DC) offset errors and LO leakage can result in errors being propagated through the signal chain. Furthermore, differences in signal paths, even within the same chip, can introduce a gain or phase mismatch of the in-phase (I) and quadrature (Q) signal, resulting in a quadrature error that can compromise signal isolation.

SDR technology offers the potential to overcome the limitations of traditional radio architectures, but few solutions can address the broader requirements associated with ADEF applications. Using the Analog Devices' [ADRV9002](#) RF transceiver, developers can easily meet the need for greater

performance and functionality with the lower SWaP demanded in these applications.

Integrated functionality delivers optimized performance with reduced SWaP

Supporting a frequency range from 30 megahertz (MHz) to 6,000 MHz, the ADRV9002 is a highly-integrated transceiver that contains all the RF, mixed signal, and digital functionality required to support a broad array of application requirements. Capable of both time division duplex (TDD) and frequency division duplex (FDD) operation, the device features separate dual-channel direct conversion receiver and transmitter subsystems that include programmable digital filters, DC offset correction, and quadrature error correction (QEC).

Within its on-chip synthesizer subsystem, the ADRV9002 features two distinct phase-

locked loop (PLL) paths: one for the high-frequency RF path and another for the digital clocks and converter sampling clocks. Finally, the device's digital signal processing block includes an [Arm M4](#) embedded processor that handles self-calibration and control functions (Figure 3).

Able to operate in either zero-IF mode or low-IF mode for phase-noise-sensitive applications, the ADRV9002 features transmitter and receiver subsystems offering complete signal chains. Each transmitter subsystem provides a pair of digital-to-analog converters (DAC), filters, and mixers that recombine I and Q signals and modulates them onto the carrier frequency for transmission.

Each receiver subsystem integrates a resistive input network for gain control that feeds a current mode passive mixer. In turn, a transimpedance amplifier converts the mixer's current output to a voltage level that is digitized by an ADC with a high dynamic range. During available transmitter slots in TDD operation or in FDD applications where only one receiver system is used, unused receiver inputs can be used to monitor transmitter channels for LO leakage and QEC, or unused receiver inputs can be used to monitor power amplifier (PA) output signal levels.

The latter capability comes into play in the ADRV9002's integrated

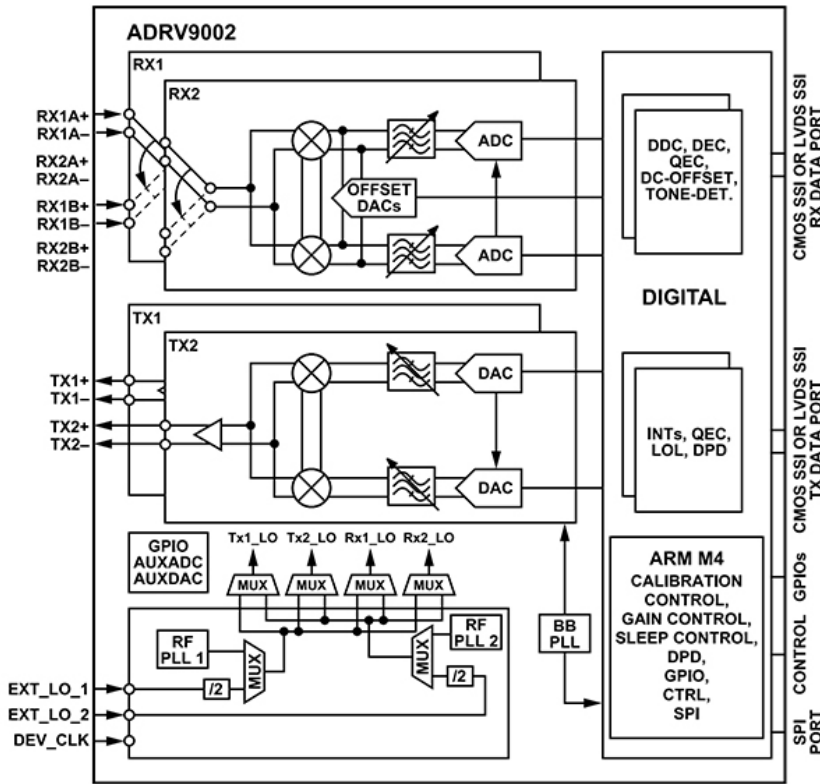


Figure 3: The ADRV9002 RF transceiver integrates dual receive (RX) and transmit (TX) subsystems. *Image source: Analog Devices*

digital pre-distortion (DPD) feature, which uses its monitored PA signal levels to apply the appropriate pre-distortion required to linearize the output. This capability enables the ADRV9002 to drive the PA closer to saturation, optimizing its efficiency.

Tuning power and performance

The ADRV9002 device provides a fully integrated solution in a 196-ball chip scale package (CSP) ball grid array (BGA), as well as minimizing size and weight for SDR ADEF communications systems. To help developers further optimize power consumption, the ADRV9002 integrates multiple features

designed specifically to help developers find a suitable balance between performance and power.

At the block level, developers can deploy power scaling on individual signal path blocks to trade reduced performance for lower power consumption. In addition, the blocks in TDD receive (RX) and transmit (TX) frames can be disabled to sacrifice RX/TX or TX/RX turnaround times for lower power consumption. To further aid the developers' ability to optimize power versus performance, each ADRV9002 receiver subsystems include two pairs of ADCs. One pair comprises high-performance sigma-delta ADCs, while the

second pair can substitute when power consumption is critical.

For applications characterized by periodic stretches of inactivity, the ADRV9002's RX monitor mode can be employed. In this mode, the ADRV9002 alternates between a minimal power sleep state and a detect state at a programmed duty cycle. In the detect state, the device activates a receiver and attempts to acquire a signal over a bandwidth and RX LO frequency programmed by the developer. If the device measures signal power level above the programmed threshold, the device exits monitor mode, and the ADRV9002's blocks are powered up to handle the desired signal.

Rapid prototyping and development

To help engineers move quickly into evaluation, prototyping, and development, Analog Devices provides extensive hardware and software support of ADRV9002-based systems.

- For hardware support, Analog Devices offers a pair of ADRV9002-based cards:
 - [ADRV9002NP/W1/PCBZ](#) for low band applications operating in the 30 MHz to 3 gigahertz (GHz) range
 - [ADRV9002NP/W2/PCBZ](#) for high band applications in the 3 to 6 GHz range

Equipped with FMC connectors, these cards support the onboard ADRV9002 with power regulation

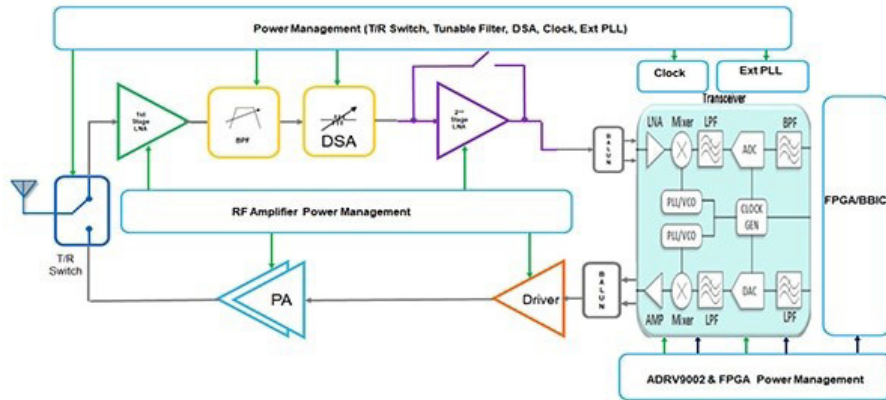


Figure 4: The highly integrated ADRV9002 transceiver enables developers to quickly implement specialized designs. *Image source: Analog Devices*

and hardware interfaces, as well as clock and multichip synchronization (MCS) distribution. The cards connect through their FMC connector to an FPGA motherboard, such as [AMD's ZCU102](#) evaluation board for power and application control.

Analog Devices provides a complete schematic and bill of materials (BOM) for its ADRV9002NP radio cards in its support package. The schematic and BOM provide an effective starting point for custom hardware development for most applications. Some applications require an additional RF front-end to meet specific signal conditioning requirements. For these applications, developers only need a few additional components to complete their design (Figure 4).

In this example, developers can quickly implement a suitable RF front-end using the following power management components from

Analog Devices:

- [ADRF5160](#) RF switch
- [HMC8411](#) low noise amplifier (LNA)
- [ADMV8526](#) digitally tunable bandpass filter
- [HMC1119](#) RF digital step attenuator (DSA)
- [HMC8413](#) driver amplifier
- [HMC8205B](#) PA

Analog Devices provides comprehensive software

development support through documentation and downloadable software packages. Developers using the development hardware mentioned above can proceed with prototyping and development based on Analog Devices' product line software or open-source software packages.

This article limits the following discussion to product line software. For more information about the open-source development methodology, see Analog Devices' ADRV9001/2 Prototyping Platform User Guide. Analog Devices stipulates that the term "ADRV9001" in the company's support documentation is meant as a family designator encompassing the ADRV9002 and other members of the ADRV9001 family. Consequently, references to ADRV9001 in the text or figures below apply to the ADRV9002 device that is the focus of this article.

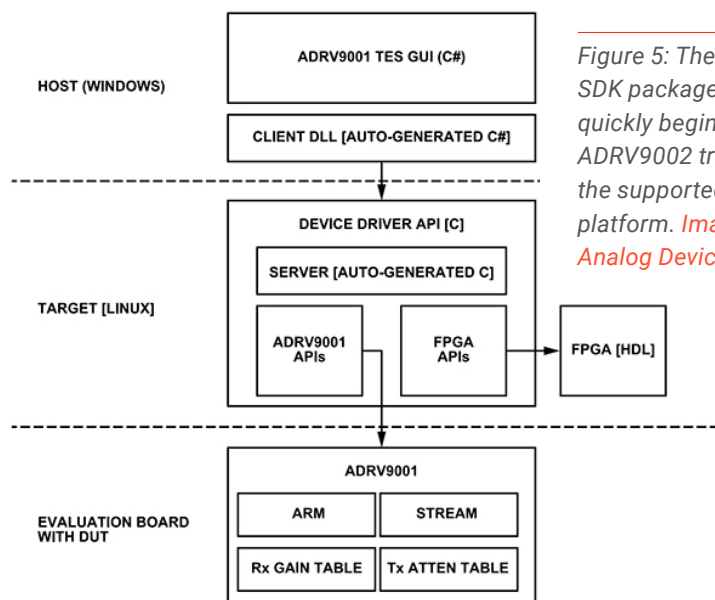


Figure 5: The TES tool in the SDK package lets developers quickly begin evaluating the ADRV9002 transceiver on the supported evaluation platform. *Image source: Analog Devices*

Using a highly integrated transceiver from Analog Devices, developers can implement SDR solutions to more effectively address these requirements

Available through Analog Devices' product line software development kit (SDK) distribution, the company's Windows-based [Transceiver Evaluation Software \(TES\)](#) tool provides an accessible starting point for quickly configuring and evaluating transceiver performance.

During evaluation and prototyping with Analog Devices' ADRV9002-based cards and AMD's ZCU102 evaluation board, the TES tool provides a graphical user interface (GUI) for configuring the hardware and observing captured data (Figure 5).

In turn, the TES tool autogenerates C# code that can be compiled to the Linux environment, MATLAB environment, or Python. The SDK provides a complete set of

software libraries and application programming interfaces (APIs), including the ADRV9001 API package developed for the AMD ZCU102 platform.

The SDK flow also directly supports migration from evaluation and prototyping with the evaluation board to the developer's custom target environment (Figure 6).

In this migration flow, the developer lets the TES autogenerate code as before. However, instead of using it directly, the developer deploys an edited version of the generated code to the target platform. In practice, the required edits are confined mainly to removing function calls that reference hardware components recognized by the TES tool but not needed in the target system. The SDK

architecture includes a hardware abstraction layer (HAL) interface between the ADRV9001 library and the developers' hardware, so developers need only provide custom code that implements the HAL interface code for their specific hardware. As a result, developers can quickly move from evaluation using the Analog Devices cards and AMD board to development for their custom target environment.

Conclusion

ADEF applications face growing challenges in an increasingly complex signal environment. Along with meeting the demand for higher performance across a wider range of frequencies, developers need to lower SWaP to support the migration of these applications to battery-powered systems. Using a highly integrated transceiver from Analog Devices, developers can implement SDR solutions to more effectively address these requirements.

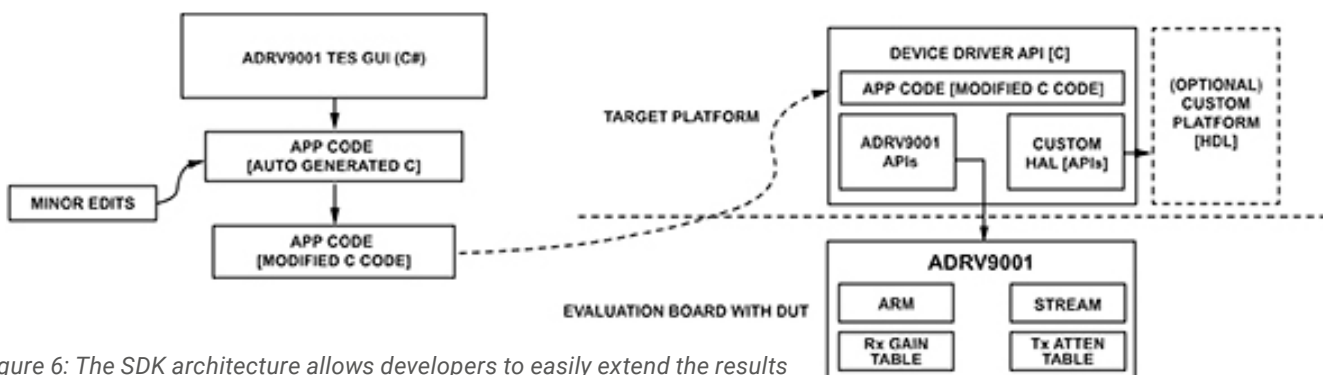


Figure 6: The SDK architecture allows developers to easily extend the results of their evaluation to their own target platform. *Image source: Analog Devices*



Why a good LNA is key to a viable antenna front-end

Written by Bill Schweber

One of the first lessons about RF and wireless links that any student learns is that antennas adhere to the reciprocity principle. This means that the transmit and receive characteristics of an antenna are identical, with no difference in attributes such as transmit or receive gain, beamwidth, or radiation patterns between the two modes. If you know the specifications of the

antenna in transmit mode, then you also know them in the receive mode. Of course, antennas for higher power transmission are often made of physically larger elements as needed to handle the power, but reciprocity still holds.

There is some research into non-reciprocal antennas using metasurfaces and metalenses, but they are in the R&D stage and not a concern here.

Reciprocity is certainly a simplifying design principle, but there is much more to transmit and receive-side antenna paths than the antenna. The transmit side has a fairly easy task as it is a deterministic function: it takes a known, relatively strong signal with defined attributes, which has passed through the power amplifier (PA), and “presents” it to the antenna. There are few unknowns

in the path except the detailed content of the signal modulating the carrier, and that is largely (but not entirely) of very little concern to the antenna.

In contrast, the receiver signal path operates in a much more difficult, random-like scenario. It must somehow locate and capture a tiny amount of RF signal power, and act as an electromagnetic (EM) field transducer to convert that power into a usable voltage. It must do this despite in-band noise and interference of various types and sources, as well some transmitter drift, and even Doppler-induced frequency shifts in some applications.

This received power is quite low, on the order of milliwatts (mW) in a few cases and microwatts (μW) in most, so the corresponding voltage created at the antenna is usually on the order of microvolts. The voltage is too small to be used directly for demodulation in most cases, so the answer is obvious: just amplify it. To get some perspective, the received signal power for GPS signals is typically between -127 and -25 decibels (dB) relative to one milliwatt (dBm), and viable Wi-Fi signals range between -50 dBm and -75 dBm.

Low SNR is the complementary problem

The amplification solution answer tells only part of the receiver story. It's not hard to amplify

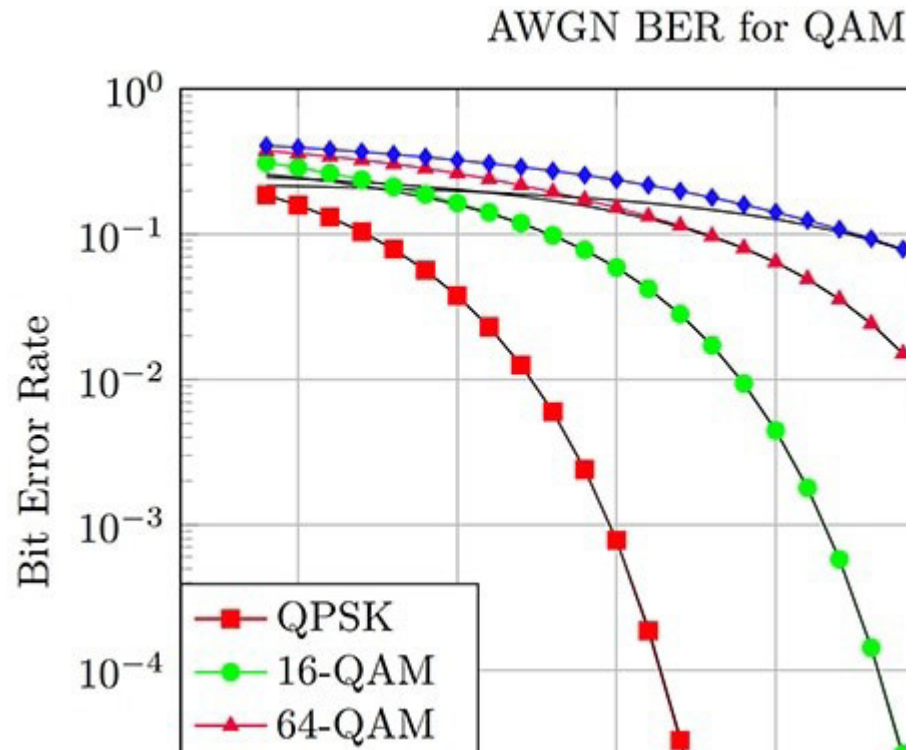


Figure 1: The standard plot of BER versus SNR reveals a great deal about system performance; note that more advanced modulation techniques such as 256-QAM can increase the effective data rate, but at a penalty in BER at a given SNR. Image source: [Julia Computing, Inc.](#)

even a microvolt signal by several orders of magnitude. However, the original signal also has noise, and what really affects the ability to demodulate and decode the received signal is its signal-to-noise ratio (SNR). Any amplification of the received signal will also amplify the embedded noise. Using a larger antenna with higher passive gain will increase the received signal power, but the received SNR will be unchanged.

One of the key metrics of system performance is its bit error rate (BER) versus SNR (Figure 1). The specifics of those curves depend

on many factors including received signal strength, SNR, and what type of error-correction code (ECC) encoding of the raw data is used at the transmitter; for this reason, the more-detailed graphs show the BER vs SNR for the raw, uncorrected bits stream as well as the corrected bit pattern (QAM = quadrature amplitude modulation).

What are some typical SNR values which result in successful demodulation with acceptably low BER? There is no universal answer, of course, but an acceptable Wi-Fi signal SNR is 20 to 40 dB, 40 to 50 dB for an old-fashioned all-analog

Why a good LNA is key to a viable antenna front-end

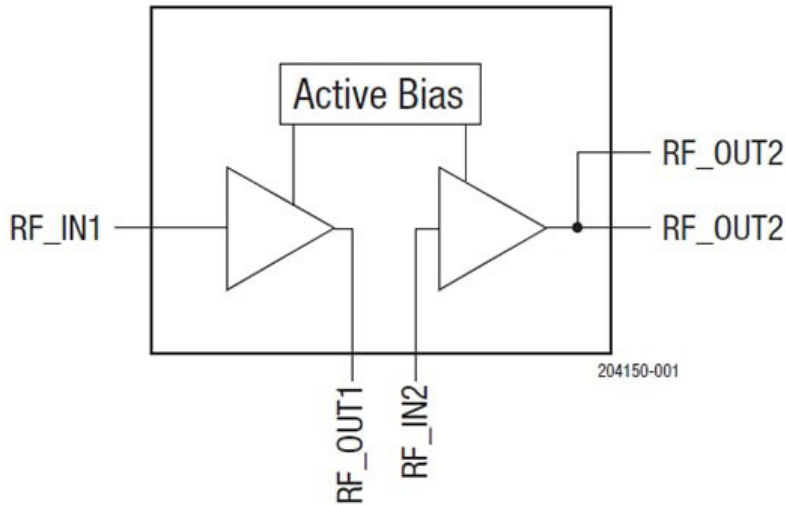


Figure 2: The Skyworks Solutions SKY67180-306LF is a two-stage, 31 dB gain LNA for 1.5 to 3.8 GHz with 0.8 dB NF; the first stage is optimized for low noise figure while the second stage provides additional gain. *Image source: Skyworks Solutions*

TV, and about the same for cellular links.

There are extreme examples, of course: signals are still being received from the Voyager 1 and Voyager 2 spacecraft, both launched in 1977 and now over 11 billion miles from Earth. These signals arrive here from their 23 watt transmitters with signal power of less than an attowatt (a billionth of a billionth of a watt) and an SNR of only a few dB. To compensate for this to some extent, their data rate is now throttled down to around 100 bits/second (bits/s), down from the several kilobits/second (Kbits/s) rate when much closer

with much higher received signal strength.

LNAs to the rescue

There's an engineering cliché that originated in the early days of "wireless" and is still true: if it wasn't for noise, the challenges of most system designs would be much, much easier. This is true of a receiver's antenna link for a simple reason. The amplifier, which is needed to "gain-up" the weak received signal, contributes its own noise to that signal, as does any interconnection cabling between antenna and receiver front-end.

Although antenna transmitter and receiver functions adhere to the principle of reciprocity, their actual challenges diverge

The need to amplify the received signal presents a dilemma. On one side, the unamplified signal is too weak to be useful; on the other hand, amplification increases the signal magnitude, but also degrades SNR and thus potential link performance. This dilemma is resolved to a large extent by choosing an amplifier that contributes as little noise as possible.

The front-end low-noise amplifier (LNA) has two parameters of primary interest: how much noise it adds to the signal, and how much gain it can provide. LNAs fabricated with highly specialized analog processors do one thing well



(provide gain with little added noise of their own) and are not suitable for non-LNA applications.

One example is [Skyworks Solutions' SKY67180-306LE](#), a two-stage, high-gain LNA for 1.5 to 3.8 gigahertz (GHz) applications such as cellular repeaters and small/macro-cell sites for LTE, GSM, and WCDMA applications, as well as S-band and C band ultra-low-noise receivers (Figure 2).

The first stage of this 16-lead QFN device uses GaAs pHEMT transistors for an ultra-low noise figure (NF), while the output stage (heterojunction bipolar transistors) provides additional gain at that frequency, along with high linearity and efficiency. The result is an LNA

with a noise floor (NF) of 0.8 dB and 31 dB gain at 3.5 GHz.

Another critical issue is where to physically place the LNA; it's obviously easier to put it with the rest of the receiver circuitry. However, this means that the unavoidable thermal noise of the cable carrying the amplified signal from the LNA to the system will be added to the unamplified signal, further reducing SNR. For this reason, even consumer applications such as very small aperture terminal (VSAT) satellite dishes put the LNA right at the focal point of the dish.

Conclusion

Although antenna transmitter and receiver functions adhere to the principle of reciprocity, their actual challenges diverge. For many RF antenna situations, a dedicated LNA is often the best or only way to boost the received signal level to a usable value while having minimal impact on SNR. Specialized LNAs are available that are tailored to specific frequency bands and with gain values that can resolve the signal level/SNR dilemma.

Related content

1. "Get the Most Out of Exotic Processes for 5G LNAs"
<https://www.digikey.com/en/articles/get-the-most-out-of-exotic-processes-for-5g-lnas>
2. "Understanding the Basics of Low-Noise and Power Amplifiers in Wireless Designs"
<https://www.digikey.com/en/articles/understanding-the-basics-of-low-noise-and-power-amplifiers-in-wireless-designs>
3. "Low-Noise Amplifiers Maximize Receiver Sensitivity"
<https://www.digikey.com/en/articles/low-noise-amplifiers-maximize-receiver-sensitivity>

References

1. Increase Broadband Speed, "[Wi-Fi Setup Guide: What is a Good Signal Level or Signal-to-Noise Ratio \(SNR\) for Wi-Fi?](#)"
2. Nordic Semiconductor, "[GPS functionality test](#)"
3. The Great Courses Daily, "["Voyager 2" Sends Messages from Interstellar Space with Minimal Signal](#)"
4. National Radio Astronomy Observatory, "[How Strong is the Signal from the Voyager 1 Spacecraft When it Reaches Earth?](#)"
5. IEEE Communications Society, "["Voyager - A Space Exploration Mission Like No Other"](#)"



Wildman Whitehouse and the twenty-five-hundred-mile-long capacitor

Written by David Ray, Cyber City Circuits

Figure 1. Whitehouse



Pioneer or pretender?

Wildman Whitehouse was a medical doctor and a self-taught electrician whose ambition ultimately led to pioneering achievements and significant failures. He put himself in the world of engineers and scientists, but he was neither. You will not find statues of this man. He was not knighted or celebrated. There are no places of honor bearing his name. Within weeks of the cable's installation, he was exposed as a fraud, a fool, and a con man. Wildman Whitehouse was a nineteenth-century Elizabeth Holmes. His 'experiments' sunk the world's first million-dollar business endeavor, The Atlantic Cable of 1858.

The story of Wildman Whitehouse is a story of unchecked arrogance, ambition, humiliation, and disgrace.

Figure 2. Wildman Whitehouse's Signature

The Atlantic Cable

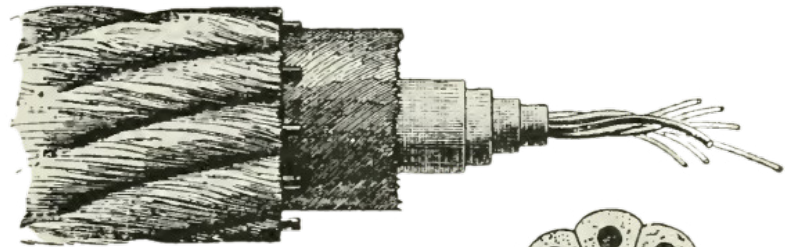
Before the trans-Atlantic telegraph cable was completed, the only way to get messages to and from Europe and the New World was by a two-week trip on a ship. The cable, laid in 1858, was twenty-five hundred miles long and the first of its kind. Submarine cabling wasn't even possible until the discovery of the material gutta-percha ten years earlier. This cable became the world's first million-dollar business venture, with the bulk of the funding coming from an American businessman named Cyrus West Field.

A working trans-Atlantic cable to communicate across the Atlantic Ocean in 1858 was the most significant technological achievement at the time, on the same scale as man landing on the moon one hundred years later.

The issue with submarine cables

The first commercial Telegraph line ran from Washington, D.C., to Baltimore, Md., in 1844. Telegraph lines were run overhead, and thousands of miles of cable were run each week worldwide.

Fun fact: Morse sent the world's first commercial telegraph from Washington DC to Baltimore, Maryland, in 1844, asking, "What hath God wrought?"



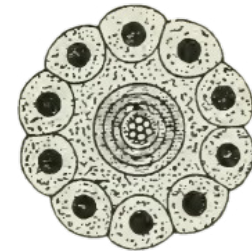
THE MAIN CABLE

Figure 3. The Main Cable

Telegraph engineers had trouble running cable underground or underwater because the dielectric insulation was never good enough. The British discovered a type of natural plastic called gutta-percha in India, which acted as a perfect insulator for undersea cables.

The discovery and effects of gutta-percha on civilization cannot be overstated. It is on the scale of discovering fire or inventing the wheel. Someday, it would make a good Retro Electro article.

The first successful submarine telegraph cable was laid in 1850, and soon after, telegraph cables were first being run underground and underwater, and a new phenomenon that seemed only to affect submarine and buried cables, called retardation (signal



propagation delay), was uncovered. Over a long distance, the submarine cables would have a delay in their signals. Something that would take seconds to transmit using above-ground cabling would take minutes over the same length of underwater cabling. Dots and dashes would be stretched out and blurred together, and if the operator transmitted too fast, the receiving operator wouldn't be able to decipher it.

Telegraphs essentially work by passing a current through a wire to cause an effect at the other end. Today, we think of telegraphs as a bunch of beeps and boops, but do you think they had speakers in the 1850s? Telegraph receivers of this time used visual mechanisms to read messages. Common methods included needle instruments, where the needle would move in response to electrical signals, or recording devices that printed symbols on paper. Whitehouse used a form of electrochemical recording that marked electrically sensitive paper. At the same time, William Thomson

developed the mirror galvanometer, which reflected light onto a scale to indicate signal strength and direction. These visual readings allowed operators to interpret messages effectively.

Longer cables start behaving like how a capacitor does when any alternating signal (frequency) is passed through it. The charged conductor would become a plate, gathering electrons towards the grounded parts of the cable. So, when the transmitter starts sending a current, the cable begins to store a charge, and when the transmitter stops the current, the cable begins to discharge, making the needle move very slowly. If the signal is too fast, sometimes the needle wouldn't move at all.

Professor Michael Faraday reported to the Royal Institution on January 20th, 1854. There, he and Werner Siemens agreed that signals could only travel around 750 miles per second along buried wires, meaning they were slower underwater. This was due to the Leyden charge, which gives submarine cables the quality of a low-pass filter. I don't think they fully grasped resonant frequencies and capacitive reactance yet.

At the time of Faraday's report in 1854, it seemed that a cable long enough to span the ocean would have such a terrible signal delay that it would not be possible to make practical or, more importantly, *profitable*.

In 1855, William Thomson (later known as Lord Kelvin) published an influential paper called "On the Theory of the Electric Telegraph." This paper introduced 'the law of squares,' which showed that signal distortion with submarine cables increases exponentially with the cable's length, resulting in significant challenges with very long-distance submarine telegraphy.

Edward Orange Wildman Whitehouse



Figure 4. Wildman Whitehouse

Edward Orange Wildman Whitehouse was born in 1816. However, only a little is known about his life prior to the 1850s. By training in trade, he was a surgeon. His contemporaries describe his character in the same way someone would describe Scrooge in *The Christmas Carol*. According to one of his peers, 'He was a gentleman of very high intellectual and scientific attainments and a

most ingenious and painstaking experimenter,' but by most other accounts, Whitehouse was arrogant, brilliant, foolish, and an incessant liar.

He attended the Royal College of Surgeons, where he won multiple awards for his work developing molds for anatomical study. After graduation, he worked as a surgeon at the Sussex County Hospital, but for some reason, he was no longer a practicing surgeon within five or ten years.

In a previous Retro Electro article, '*Ethereal Fire Considered*,' we wrote about the intersection of medicine and electricity. In the late 18th century and early 19th century, how electricity affects the human body wasn't fully understood. Electricity couldn't even be put to practical use until the invention of the Leyden Jar in 1745. Before the 1840s, many people reasoned that electricity was deeply connected to God and health. These thoughts date all the way back to Aristotle and didn't really change until the middle of the nineteenth century.

It's easy to consider that Whitehouse could've been a mad doctor who used electricity in his treatments. They surely would have taught him some electrical therapies when he attended college. His reckless nature could have led to grave injuries, forcing him to resign as a doctor. He took his electrical knowledge from the medical field and brought it

to the new and exciting world of telegraphy. Whitehouse had little or no formal training in engineering, mechanics, or natural philosophy. Still, he managed to be made the chief electrician of the Atlantic Telegraph Company with a mixture of ambition and confidence.

Electrotherapy at this time used a varying range of voltages. The idea was that if lower voltages didn't offer a remedy, higher voltages would, as long as you did it in a way that didn't kill the patient. If Whitehouse was a practitioner of electrotherapy, he would have been familiar with winding his own coils and making a generator. *This is important to remember later in the story when he uses high voltages on the cable.*

In 1850, Whitehouse met with John Watkins Brett, a British businessman interested in entering the booming field of telegraphy. J. W. Brett and his brother, Jacob Brett, registered a company a few

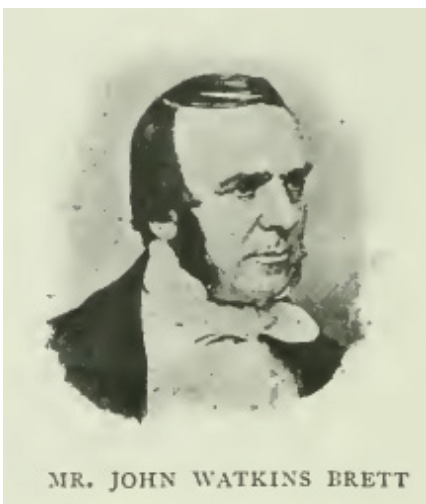


Figure 5. J.W. Brett

years earlier for a trans-Atlantic telegraph cable named 'General Oceanic Telegraph Company.' Brett hired Whitehouse to research various telegraphy-related topics, focusing on long-distance wires. Whitehouse developed his own test equipment, methods, and apparatuses.

During this time, Whitehouse produced a few patents. The first was in 1853 for a type of chemical telegraphy. In this method, a machine rolls carbon paper over a device called 'the manipulator,' which applies shocks to the paper, leaving an intelligible mark. When used effectively, this method should make communication easier and more efficient for both the operator and the receiver.

Charles Bright

While conducting research for Brett, Whitehouse met Charles Bright, the twenty-one-year-old chief engineer of the Magnetic Telegraph Company. Charles Bright, with his brother Edward, started the company in 1852 at the age of twenty and had tremendous

Figure 6. Chemical Telegraph. The electro-chemical decomposition printer from Whitehouse's 1853 patent.

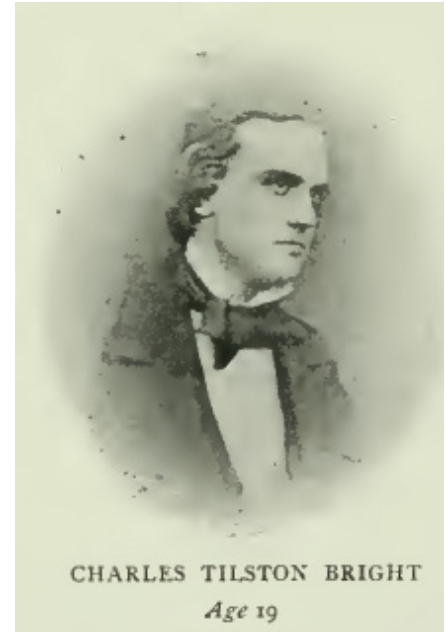
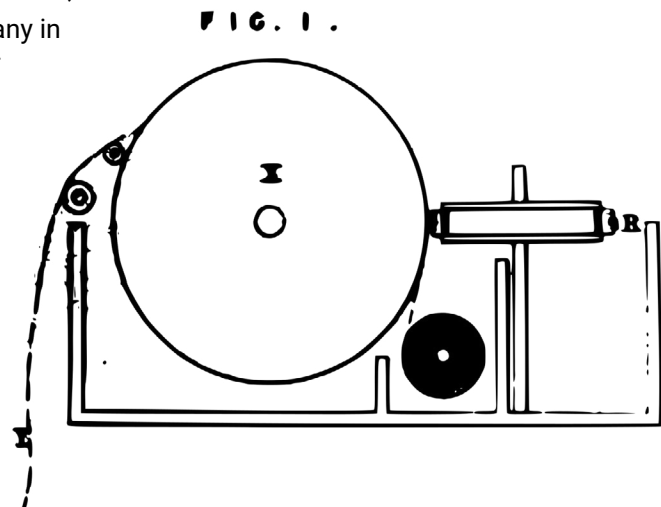


Figure 7. Charles Bright

success, with lines running all over the United Kingdom and Ireland. By the time Bright entered into the story, he had already made significant contributions to submarine cable technology.

The longest cable Whitehouse could test was a couple of hundred miles long, but with the help of Charles Bright, he could have

different telegraph stations connect their lines, eventually achieving 600 miles of cable, much of which was underground and underwater.

Whitehouse and Bright studied and tested the cable to determine how fast a signal could travel in miles per second. Overhead telegraph wires were found to have a transmission speed of about sixteen thousand miles per second. In 1854, Bright's brother, Edward Bright, reported on experiments showing that underground cable signals do not exceed one thousand miles per second, demonstrating the cable's ability to hold a Leyden charge.

This was caused by the propagation delay discussed earlier. The fact is that a commercial telegraph line spanning the Atlantic Ocean could not be profitable at that speed.

Charles Bright would become the Chief Engineer of the Atlantic Telegraph Company. In later writings, Whitehouse says that Charles Bright suggested they collaborate on an Atlantic telegraph line together, with Bright himself proposing that Whitehouse take the "larger share of anything that might result from our union." If true (it may not be), this portrayal highlights Bright's trust in Whitehouse and willingness to grant him the leading share in any rewards, aligning with Whitehouse's ambition and persuasive nature.

Wildman to save the day

DigiKey

The following year, in 1855, at the British Association for the Advancement of Science, Whitehouse gave his first report, 'Experimental Observations on an Electric Cable,' making his introduction to the world of electrical science. Remember, while Dr. Whitehouse was brilliant, he would have been highly peculiar, esoteric, and arrogant to anyone around him.

In this report, he explains how the cable could discharge much faster using large inductive coils and alternating currents. These tests were done on cables manufactured and stored in coils for installation in the Mediterranean and Newfoundland and amounted to 1,125 miles in length. He explains that current generated by a chemical battery simply cannot perform as well as currents generated by magneto-electric generators, which, according to his claims, perform three and a half times better than the former, with speeds up to six thousand miles per second.

This was in considerable contrast to what Thomson and Faraday had said earlier and contradicted the law of squares. While Thomson reported that it would be very difficult, if not impossible, to operate a submarine cable long enough to travel to the Americas, Whitehouse spoke of it as if it could be trivial if they did it the way that he proposes with his patented equipment.

Thomson was a professor of Natural Philosophy at the University of Glasgow and much more qualified to answer this question. Yet, he did not have an answer that people wanted to hear. Within weeks, Whitehouse's report made its way to the desk of Cyrus West Field in New York City.

The year before, Latimer Clark gave a report proposing that the term 'ohm' should be used for electrical measurements. You can read more in the Retro Electro article 'Ohm's Day.' (Link: <https://emedia.digikey.com/view/639112496/21/>)

Cyrus West Field

Cyrus West Field was an American businessman who made his fortune in the paper industry before turning his attention to the ambitious goal of connecting the continents with a cable. Born in 1819 in Massachusetts, Field worked his way up in business, eventually establishing himself

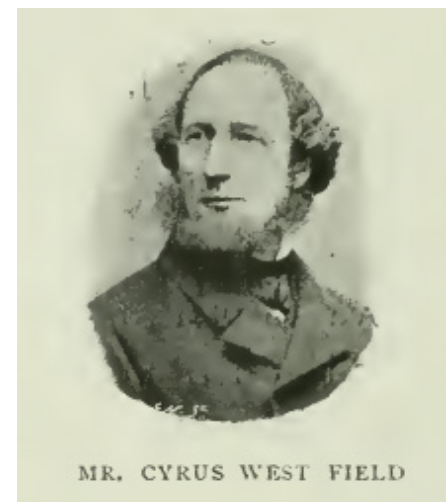


Figure 8. Cyrus West Field



NEWFOUNDLAND TELEGRAPH STATION, 1855

Figure 9. Newfoundland Telegraph Station

as a successful merchant in New York City. Never to be found bored, by the early 1850s, in his early thirties, he had accumulated such substantial wealth that he wanted a new challenge.

As a young man, he was glad to take on great risks in the name of progress, investing money in businesses during the early industrial age. In 1854, Field was approached by Frederick

Gisborne, a Canadian engineer attempting to lay a telegraph line across Newfoundland. Inspired by the broader potential of linking North America to Europe via an undersea cable, Field took on the project, quickly realizing its global significance and monumental challenge.

In 1856, after assembling a group of investors he called the "Cable Cabinet" and rallying American

and British support, Field founded the Atlantic Telegraph Company alongside J. W. Brett, chief engineer Bright, and Whitehouse as chief electrician. This company was created to manage the unprecedented task of laying a telegraph cable across the Atlantic Ocean. Field worked tirelessly to secure funding, coordinate logistics, and win political and public backing for the project.

The Atlantic Telegraph Company

"It was not till 1856 ...that the enterprise had any existence in England. In that summer, I went to London, and there, with Mr. John W. Brett, Mr. Charles Bright and Dr. Whitehouse, organized the Atlantic Telegraph Company." – Cyrus West Field

According to Whitehouse, he spent every waking moment for the next two years working on solving the trans-Atlantic cable problem. He used his knowledge to design an elaborate system of relays, spark



Figure 10. The Main Cable 2

gaps, and coils to develop what he felt was the state of the art in long-distance telegraphy. Newspapers of the day, claim that he was able to talk himself into an annual salary of £1,000 a year (\$175K in 2024), and once the telegraph was up and running, he would receive a £10,000 (\$1.75M in 2024) salary a year. Certainly, this was all contingent on his patented equipment being *necessary* for the line to work.

“The coils are used in pairs and consist of large hollow iron cores, 5 feet in length, and each wound with the following lengths of copper wire: –first, with about 11,000 yards of No. 20 gauge silk-covered copper wire, for a secondary circuit, insulated with wax paper between the layers, and hermetically enclosed in gutta-percha. And over this a primary circuit of thick wire, No. 14, consisting of 24 parallel circuits of about 100 yards.” – Whitehouse on the coils used in his design.

Two different manufacturers were used to make the cable. There were no standards or proper testing procedures. According to Whitehouse, he tried to test the cable many times throughout its manufacture but was unable to. The cable took a year to make, and it was placed on two different ships. Whitehouse could never fully test the cable connected from end to end.

Writer’s note: according to a biography of Charles Bright by his brother and son, Whitehouse was not a founding member of the Atlantic Telegraph Company, but every other account the writer can find says he was. He states it was just Bright, Cyrus W. Field, and J. W. Brett, and then Whitehouse joined later.

Over the next two years, there were three attempts to get the cable across.

Attempt 1: August 1857

The first attempt to lay The Atlantic Cable began in August 1857. It was marked by high hopes, with both British and American ships, HMS Agamemnon and USS Niagara, carrying out the mission. They both carried half of the cable, starting in Ireland and heading to Newfoundland. This effort faced numerous weather-related and technical difficulties, including problems with the cable’s insulation and the challenging conditions of the deep ocean, leading to the cable breaking after about 380 miles. This initial setback revealed just how complex and demanding the task would be.

Attempt 2: June 1858

The second attempt began in the early summer of 1858. They used the same cable left over from the 1857 attempt but left it outside in the Irish weather for several months





Figure 11. On June 20th, 1858, a storm broke the cable of the second attempt.

working on the line with his own patented tools, using his special coils and heavy relays. He didn't send any report to the directors for a week, which made everybody nervous. His excuse was that he was just adjusting things when, in reality, he was using bigger coils, batteries, and generators.

They were receiving signals soon after, but they couldn't make out any intelligible messages. They both worked independently to try

to get it online. After a few days, though, Thomson had to leave to return to the University of Glasgow to teach. He had not been able to see his classroom since May. Before he left, Whitehouse told him that he suspected that there was a fault in the cable a few miles in the harbor. The water was shallow, and he wanted to go and pull it up to check it. Thomson told Whitehouse that there was no evidence for this and that if there was a fault, it

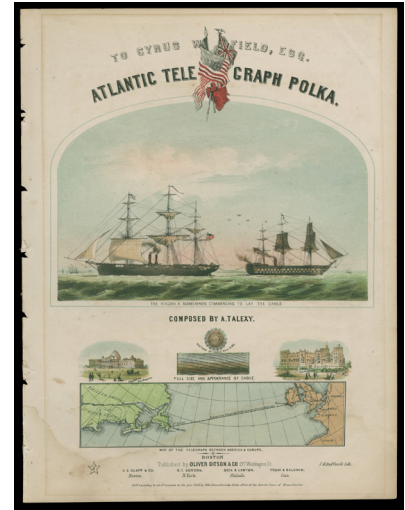
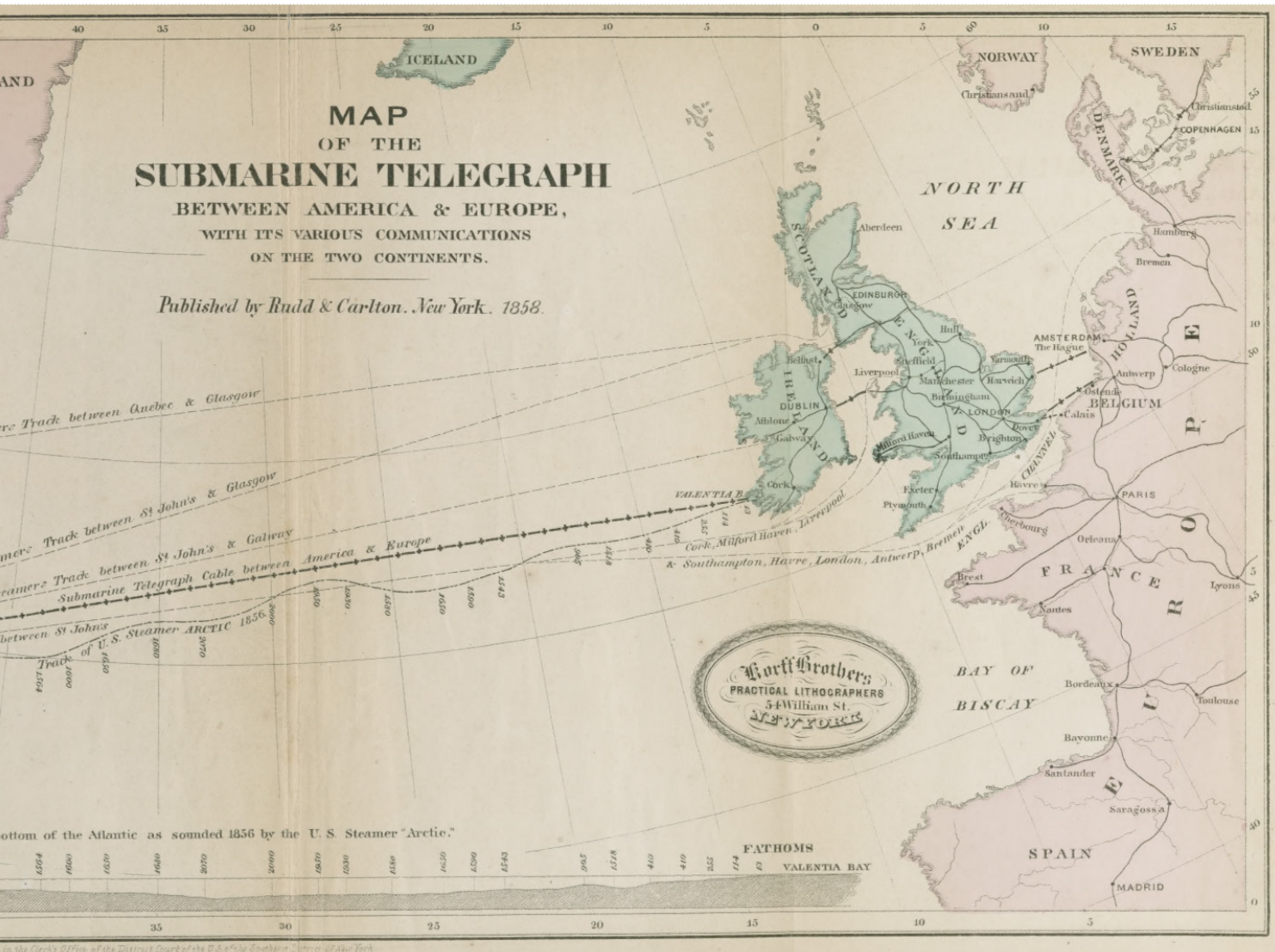


Figure 13. Atlantic Telegraph Polka



was probably about three hundred miles in, where the ocean starts to get very deep. In one of the first reports that the board received from Whitehouse, he proposed that they raise the cable to look for a fault. The board quickly and strictly ordered that he must not attempt this. At the same time, they sent a skilled telegraph operator named Mr. France to assist Whitehouse, but when he arrived, he was turned away and refused admission by Whitehouse. After a few days of evasive responses, the board discovered that Whitehouse had raised the cable, cut it open, spliced it back together, and tied it to a buoy in the harbor.

The Queen's message

"From Her Majesty the Queen of Great Britain to His Excellency the President of the United States. The Queen desires to congratulate the President upon the successful completion of this great international work, in which the Queen has taken the greatest interest. The Queen is convinced that the President will join with her in fervently hoping that the electric cable, which now already connects Great Britain with the United States, will prove an additional link between the two nations, whose friendship is founded upon their common interest and reciprocal esteem. The Queen has much pleasure in thus directly communicating with the President and in renewing to him, her best wishes for the prosperity

of the United States." – The first message from Queen Victoria to President Buchanan took over sixteen hours to transmit and verify.

The first message from Queen Victoria to President Buchanan was sent on the 16th of August. On this day, Whitehouse was the operator that sent the inaugural message across the Atlantic Ocean. It was roughly 100 words and, according to Whitehouse just a year earlier, would take minutes to send. It took over sixteen hours to transmit. The majority of this was caused by the signal delay that Thomson warned about, but Whitehouse said that would be fine in 1855. Eventually, they removed Whitehouse's coils and equipment and used Thomson's Mirrored Galvanometer and batteries.

Whitehouse must have put on

some show because The Atlantic Telegraph Company board fired him the next day. They then sent this message to Thomson at the University of Glasgow, begging him to return and correct the chaos left by Whitehouse.

'Dear Sir, You are hereby authorized and empowered to take charge and possession (until further arrangements can be made) of this Company's office and electrical apparatus at Valencia and to issue, in respect to the adjustment and working of the instruments, such instructions as you may deem best. It is also hereby ordered and authorized that no person, whatever is to be allowed, on any pretense, to enter the Company's electrical department without your special order and permission. We are, dear

Figure 14. Eighth Wonder



*Sir, Yours truly, C. M. Lampson,
Vice-Chairman.' – A message from
the board of the Atlantic Telegraph
Company to Professor Thomson,
the day after Whitehouse was fired
(18 Aug 1858)*

Newspapers covered the event as the eighth wonder of the world. Parades were held all over. More than anybody else, Cyrus West Field was held up as a saint. It was heralded as the greatest technological event since the invention of the wheel. Queen Victoria knighted Charles Bright within a week of its completion.

Unfortunately for the life of the cable, Whitehouse was instilled with a conviction that currents of very high strength were the best for signaling, and he had enormous induction coils. Five feet long, yielding electricity estimated at about two thousand volts. Whitehouse would constantly increase the power to no purpose. The insulation could not bear the strain, and the signals gradually failed.

The cable is a failure

The last *complete* message received was on September 1st, 1858, at a rate of four letters a minute, starting one the largest *failure analyses* in history. Seven hundred thirty-two messages were sent across the cable before it was abandoned and considered hopeless before the end of the year.

What was celebrated worldwide soon became dread as the realization sat in that the cable wasn't going to work anymore. Investors were quick to pull out. Nobody wanted to work on the project anymore, and newspapers blasphemed Whitehouse's name in black and white all over England, Europe, and the United States. Whitehouse was the center of all the blame. Despite all the negative attention, he continued to try to get his job back. It is not clear if he was fighting to get his job back or if he was fighting to get his £10,000 a year salary.

In an issue of Harper's Weekly, they tell the story of how Whitehouse has to be physically thrown out of the telegraph station. *"We must observe at the outset that any proposition coming from Mr. Whitehouse should be received with caution. By skillful management, at the outset of the telegraph enterprise, Mr. Whitehouse contrived to obtain from the managers an engagement as chief electrician and in the event of the success with the cable, a pleasant salary of \$50,000 a year. When shortly after laying the cable, it became evident that Mr. Whitehouse could not make it work, it was actually necessary to use force to disengage his grip on the enterprise and its instruments. He was turned out of the Valencia Telegraph house with violence and contumely. When therefore, he sets forth a scheme that conditions precedent of which is that he should be reinstated*

in possession and authority, caution should be exercised and entertaining it."

Whitehouse's defense

In a lengthy article published in the London Morning News (Sept 20, 1858) titled 'The Atlantic Telegraph Cable,' Whitehouse opens, claiming that success was unexpected, which is strange for the Chief Electrician for the most expensive technological endeavor in history to say. His rebuttal is dated September 18, 1858, within weeks of the cable's failure. In it, he tells the entire story of The Atlantic Cable, from the first time Professor Samuel Morse published the idea in 1842 to the most recent failure he was connected to.

*"The excitement, consequent upon the **unexpectedly successful** laying of the Atlantic Cable, and the realization of electric communication with America— followed as it has been at so early a time by a painfully ominous silence of many days — leads me to believe that a succinct outline of the scientific part of the undertaking would be valued."* - Whitehouse

In October, he filed a patent titled 'A New (or Improved) Mode of Protecting Insulated Telegraph Wires,' attempting to demonstrate a higher knowledge of the problem, but it didn't work. The following months had to be hard for Whitehouse. Newspapers worldwide were printing libelous



opinions and destroying any reputation that he may still have.

He was not aboard the ships

Whitehouse didn't go aboard the ships as they laid the cable. This came up as one of the reasons he was fired. He claims it has to do with illness and health issues, and they were okay with him not attending before this crisis. They argue that, as chief electrician, he should have been on the boat, and that was one of the reasons he was hired for. If he had been present, there might not have been a crisis, to begin with.

"The Directors now, for the first time, put forward as a plea for my dismissal, my inability from illness to accompany the ships, one of the duties for which it is said I was "engaged" and "paid," and which now is called "by far the most important," though at midsummer no sort of objection was offered to my remaining at home and I was even confidentially advised by their secretary to do so." - Whitehouse

No proper test procedure prior to deployment

Whitehouse argues that there was

no way for him to test the cable as it was being produced properly. The cable was being made by two different manufacturers, far apart from each other. Testing during manufacturing is essential, especially when you're trying to develop a new groundbreaking technology.

In future testimony, people will argue that he was given ample time to test and he did test. He was there testing. Perhaps he couldn't do the test that he felt he needed to, but that could have been due to a lack of effort or energy on his side. If he had been easier to work

with, he could have had a team of assistants and technicians at his whim, but he could not manage to keep a team together.

With all this said, it is undeniable that he could not test the entire length of the cable before deployment. The cable existed on two different ships and it wasn't going to be fully connected until the installation. In this way, he is absolutely correct.

Unauthorized repair

After he was left alone with The Atlantic Cable, after Thomson left, he went and pulled the cable up and cut it open, despite being explicitly told not to. This is a pride and arrogance problem. A total inability to follow another leader and do what he is told. There is not excuse for this.

Environmental damage while in storage

The cable was manufactured with the gutta percha as an insulating material. Gutta-percha is a natural latex obtained from the sap of certain trees in Southeast Asia. It is relatively stable and resistant to water and electrical conductivity, but it can degrade when exposed to heat and environmental factors over time. Heat softens the material, leading to the deformation of the insulation. Prolonged exposure to sunlight and ultraviolet radiation

can also cause it to become brittle, leading to cracks and reduced effectiveness. Additionally, gutta-percha is susceptible to oxidation, which can accelerate degradation when exposed to an oxygen-rich environment.

After the failure of 1857, the cable was stored on the docks in Ireland, sitting for nearly a year. So, this way, he is absolutely correct. It is unreasonable to expect twenty-five hundred miles of cable to sit in the environment for a year and be perfectly fine afterward.

Hasty construction and manufacture

A cable of this magnitude had never been constructed before. The shareholders rushed the cable to accelerate the path to profits. Everyone argued that the cable was perfect until Whitehouse got his hands on it. Thompson does come to his defense here, suggesting that there could be damage three hundred miles in.

One thing is clear: Whitehouse did not create the damage seen in the picture below from the Telegraph house in Ireland. Look, and

you'll see the center conductor is very far from the center. Having the cable be like this anywhere along the twenty-five hundred miles would cause damage with higher voltages. If the cable was constructed the way that it was supposed to be, there is a chance that Whitehouse might not have damaged the cable, but that's not what happened.

Coiling of the wire

The first two attempts had two ships start in Ireland with the plan that when one finished paying out its cable, the second would splice in and continue on the trip, bringing its cable with it. That was always the plan until the third attempt. This time, they met in the center, spliced together, and then went to their respective shores. This worked, but the shielding was twisted in a way that allowed for the cable to be spliced together in the first two attempts. When they spliced it together in the center and moved out, the twists unraveled each

other because the cable wasn't designed to go that way.



Figure 16. Damaged cable, a cross-section of the original cable showing a failure point.

The inquest

Not long after the cable's failure, the Queen of England commanded an investigation called the *'Joint Committee to Inquire into the Construction of Submarine Telegraph Cables.'* The regular players were there: John W. Brett, Sir Charles Bright, Latimer Clark, William Thomson, and even Wildman Whitehouse, along with a few dozen other scientists and engineers.

Whitehouse's interrogation took place on the 15th of December in 1859. The interview must have taken place all day because the record shows that he was asked two hundred and seventy-five questions. In the interview, he explained that he had performed experiments some years earlier on cable bound for the Mediterranean and Newfoundland. Each cable was one hundred sixty-six miles long, and he could use the multiple conductors in each one to loop them back and make a whole length of two thousand miles. There really was no way to do any kind of proper

Each cable was one hundred sixty-six miles long, and he could use the multiple conductors in each one to loop them back and make a whole length of two thousand miles. There really was no way to do proper experiments on two thousand miles of conductor that were coiled and wound together

experiments on two thousand miles of conductor that were coiled and wound together.

While Whitehouse did extensive testing on telegraph cables, much of it seems to have been in scenarios that could not account for the challenges of submerged cables under real oceanic conditions. His experiments, conducted chiefly on coiled and lab-bound cables, did not address or prepare for the practical issues that could arise when the cables were submerged in deep-sea environments.

They all knew this. They knew that coils had properties that submarine cables didn't, and this was well documented for years before the company's organization. The results of these experiments, which they're discussing in this inquiry, should have minimal bearing on the failure, but they don't. It just doesn't seem like he did the proper testing, and it is not clear that he could have.

The ruined legacy

The ultimate failure of the cable was attributed to several factors. Faulty joints, insulation defects, poor testing protocols, and, critically, the use of high-voltage induction coils by Whitehouse.

Another attempt would not be made for another nine years. This wait was primarily because of the American Civil War. Still, Whitehouse was blamed for this because the second cable wouldn't have been needed if Whitehouse hadn't destroyed the 1858 cable. This break was a blessing, though. After all, it allowed Bright and Thomson to take the time to better understand transmission lines. Before, they were far too hasty and cut as many corners as possible.

Following he continued in his world of tinkering and inventing. Overall, there are sixteen patents to his name. He patented things from the seats in public carriages and vehicles to improvements on roller skates, which look like a predecessor to proper roller blades.

Whitehouse played a significant role in damaging the cable but was set up for failure from the beginning. He lacked accountability, often dismissing or ignoring problems rather than addressing them proactively. Appointing Whitehouse to a leadership role was a critical mistake. The outcome may have been different if he had been placed in a junior position under a more



Figure 17. *The Atlantic Cable*

experienced leader like William Thomson. Additionally, the failure should be attributed to everyone involved, given the insufficient quality control and lack of unified direction. This story highlights the importance of speaking up when something seems wrong and the dangers of a lack of collaboration.

Whitehouse alienated those around him, including some of the most brilliant minds of his time, due to his arrogance and unwillingness to consider other perspectives. Ultimately, the project's failure was a collective one, reflecting poor decisions, inadequate oversight, and ineffective teamwork.

The writer acknowledges that Bill Burns' and Allan Green's work at Atlantic-Cable.com was instrumental in much of the research. Bruce J. Hunt's research and writing were very appreciated resources.

1816

Birth of Edward Orange Wildman Whitehouse in Melksham, Wiltshire.

1848

Discovery and application of gutta-percha for use with submarine telegraph cables.

1853

Whitehouse's first patent is filed, 'Improvements in effecting Telegraphic Communications.'

1855

Whitehouse gives his first report to the British Association for the Advancement of Science.

1857

Initial attempts to lay the trans-Atlantic cable; technological and environmental challenges encountered.

1842

Professor Morse first publishes the idea of a trans-Atlantic cable.

1850

The first submarine cable was laid.

Whitehouse begins his electrical experimentations.

1854

Whitehouse met Charles Bright while Bright worked for the Magnetic Telegraph Company.

1856

The Atlantic Telegraph Company is formed.

Extensive testing on long-distance telegraph lines, preparing for the trans-Atlantic challenge.

Suggested reading

1. 'History of the Atlantic Telegraph' by H. M. Field
2. 'Edward Orange Wildman Whitehouse' by Bill Burns
<https://atlantic-cable.com/Books/Whitehouse/eoww.htm#gsc.tab=0>
3. 'Wildman Whitehouse's Telegraph Patents' by Steven Roberts
<https://atlantic-cable.com/Books/Whitehouse/Patents/index.htm>
4. 'Wildman Whitehouse's Patents' compiled by Steven Roberts and Allan Green
<https://atlantic-cable.com/Books/Whitehouse/Patents/index.htm>
5. 'Scientists, engineers and Wildman Whitehouse: measurement and credibility in early cable telegraphy' by Bruce J. Hunt
<https://atlantic-cable.com/Books/Whitehouse/BJH/index.htm#gsc.tab=0>
6. Papers Presented at the British Association for the Advancement of Science of 1858 by Wildman Whitehouse
<https://atlantic-cable.com/Books/Whitehouse/BA1858/index.htm#gsc.tab=0>

7. Evidence of Wildman
Whitehouse, 15 December 1859
<https://atlantic-cable.com/Books/1861JCR/Whitehouse/index.htm#gsc.tab=0>
8. Reply to the Statement of the Directors of the Atlantic Telegraph Company by Whitehouse
<https://atlantic-cable.com/Books/Whitehouse/index.htm#gsc.tab=0>
9. 'The First Trans-Atlantic Cable' by Becky Little
<https://www.history.com/news/first-trans-Atlantic-telegraph-cable>
10. 'Experimental Observations on Submarine Electric Cables' by Whitehouse in 1855
<https://atlantic-cable.com/Books/Whitehouse/BA1855/index.htm#gsc.tab=0>
11. 'Report of the Joint Committee Appointed by the Lords of the Committee of Privy Council for Trade and the Atlantic Telegraph Company to Inquire into the Construction of Submarine Telegraph Cables' by the Great Britain Privy Council Committee for Trade (1861)
https://www.google.com/books/edition/Report_of_the_Joint_Committee_hl=en&gbpv=0

1858

The trans-Atlantic cable was successfully laid, and the first messages were exchanged across the Atlantic, failing three weeks later.

Charles Bright is knighted.

Whitehouse is fired.

November 1858

Whitehouse was dismissed from the project due to the cable's failure due to his high-voltage methods.

1861

Whitehouse is a paid consultant for a telegraph cable going for Malta to Alexandria.

1866

The second trans-Atlantic cable was successfully laid using the 'Great Eastern' under Thomson's guidance.

William Thomson is knighted, becoming Lord Kelvin.

Sept 22-29, 1858

Whitehouse gives five presentations at the British Association for the Advancement of Science

December 1859

Gave evidence before a committee of the House of Lords investigating the Atlantic Telegraph Company.

1865

Another attempt was made to lay a trans-Atlantic cable, but the cable broke and fell into the ocean.

1870

Whitehouse dies.

1876

Alexander Graham Bell invents the telephone.

How to quickly leverage Bluetooth AoA and AoD for indoor logistics tracking

Written by Jeff Shepard





Real-time asset tracking in warehouses and factories is an important aspect of Industry 4.0. Various technologies are available for deploying Real-Time Location Services (RTLS) for asset tracking and improving logistics systems. Global Positioning Systems (GPS) are widely used for outdoor RTLS implementations, but the signals are not always available inside buildings. Wi-Fi is another choice, but it tends to have limited accuracy, requires significant power, and can be costly to deploy. Radio-frequency identification (RFID) is low power and has good accuracy but tends to be expensive. Industry 4.0 RTLS installations are increasingly turning to Bluetooth 5.1 direction-finding techniques because they combine high precision indoor positioning plus low power consumption, low cost of Bluetooth hardware, and low cost of deployments.

It can be tempting for developers to design Bluetooth RTLS systems from scratch. Unfortunately, obtaining the radio frequency (RF) in-phase and quadrature (IQ) information of the angle-of-arrival (AoA) and angle-of-departure

(AoD) data required to calculate the position of a transceiver from the RF signal is challenging and requires the integration of multiple antennas. Even if the AoA and AoD data can be captured, location calculations can be complicated by numerous factors, including multipath propagation, signal polarization, propagation delays, jitter, noise, and more, before the location of the item being tracked can be accurately determined.

Instead, designers can turn to Bluetooth wireless systems on chips (SoCs), RF modules, and antennas for use in Industry 4.0 RTLS applications. This article briefly reviews the performance tradeoffs of the various RTLS technology choices and describes how Bluetooth AoA and AoD location is implemented. It then presents Bluetooth SoCs and RF modules that include the software needed to quickly implement AoA and AoD-based RTLS, as well as related antennas from [Silicon Labs](#) and [u-blox](#). Evaluation kits that can further speed time to market are also presented.

The most commonly used indoor RTLS technologies are

Designers who can select from SoCs and modules that include the software needed to quickly implement the complex software required to deploy Bluetooth AoA and AoD

implemented using Wi-Fi and Bluetooth (Table 1):

- Wi-Fi fingerprinting uses a database of the location and base station ID (BSSID) of each Wi-Fi access point (AP) in a building. An asset tag scans the Wi-Fi environment and reports the list of Wi-Fi APs and their associated signal strengths. The database from the survey is then used to estimate the tag’s likely position. This technique does not support high-accuracy RTLS
- Wi-Fi Time of Flight (ToF) is more accurate. It measures the time it takes for Wi-Fi signals to travel between devices. ToF requires a dense deployment of APs to improve the accuracy of RTLS. Both ToF and fingerprinting have high device costs and high energy requirements

- Bluetooth received signal strength indicator (RSSI) supports RTLS by enabling devices to determine their approximate distance from nearby Bluetooth beacons by comparing the received signal strength with known beacon positions. RSSI uses less energy and is lower cost than Wi-Fi fingerprinting or ToF, but it has limited accuracy. Its accuracy can be further reduced by environmental factors such as humidity levels and robots, or people moving around a facility and interfering with the Bluetooth signal levels
- Bluetooth AoA is the newest and the most accurate indoor RTLS technology. In addition to providing high accuracy, it uses relatively little power and is low

cost. However, it’s more complex to implement compared with the other alternatives

Bluetooth AoA and related AoD, RTLS solutions rely on antenna arrays to estimate the position of an asset (Figure 1). In an AoA solution, the asset sends a specific direction-finding signal from a single antenna. The receiving device has an antenna array and measures the signal phase difference among the various antennas caused by the differing distances of each antenna from the asset. The receiving device obtains IQ information by switching between the active antennas in the array. The IQ data is then used to calculate the location of the asset. In an AoD solution, the locator beacon to which the location is

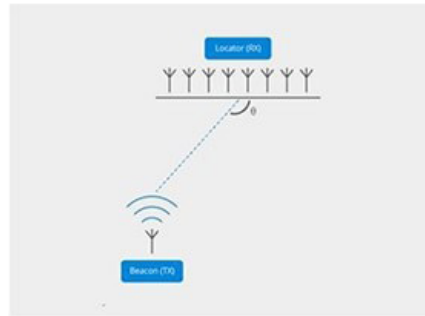
| | Wi-Fi fingerprinting | Wi-Fi time-of-flight | Bluetooth RSSI | Bluetooth AoA |
|-------------------|----------------------|----------------------|----------------|----------------|
| Accuracy | 10 m | 1 m to 2 m | 5 m to 10 m | 0.5 m to 1.0 m |
| Power consumption | High | High | Medium | Low |
| Installation cost | Low | Medium | Low | Medium |
| Device cost | High | High | Low | Low |

Table 1: Indoor RTLS can be implemented using various Wi-Fi and Bluetooth techniques that provide tradeoffs between accuracy, power consumption, and cost. Table source: u-blox

being determined transmits the signal using multiple antennas in an array and the receiving device has a single antenna. The receiving device uses multiple signals to determine the IQ data and estimate its position. AoA is often used for tracking the position of assets, while AoD is the preferred technique to enable robots to determine where they are in a facility with good accuracy and low latency.

The basic concept for AoA-based RTLS tracking is straightforward: $\theta = \arccos \left(\frac{\text{phase difference} \times \text{wavelength}}{2 \pi \times \text{distance between the antennas}} \right)$ (Figure 2). Real-world implementations are more complicated and need to account for signal propagation delays caused by environmental variables, multipath signals, varying signal polarization, and other factors. In addition, when antennas are used in an array, they can experience mutual coupling and affect each other's responses. Finally, it can be quite challenging to develop the algorithms needed to take all of these variables into account and efficiently implement them in a time-critical solution in a resource-constrained embedded environment. Fortunately for developers, complete Bluetooth AoA and AoD solutions include IQ data collection and preprocessing, multipath components suppression, compensation for environmental factors, and mutual coupling between antennas.

Angle of Arrival (AoA)



Angle of Departure (AoD)

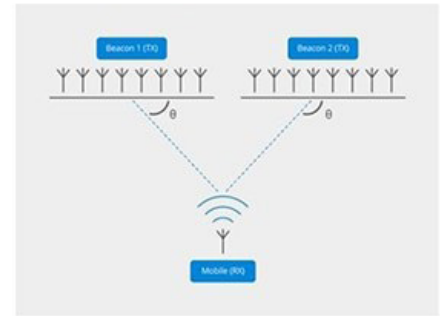


Figure 1: Antenna arrays form the basis for Bluetooth AoA and AoD RTLS implementations. *Image source: Silicon Labs*

SoCs for Bluetooth AoA and AoD

Developers can turn to SoCs such as the [EFR32BG22C222F352GN32-C](#) from Silicon Labs to implement Bluetooth 5.2 networking and AoA and AoD. This SoC is part of the EFR32BG22 Wireless Gecko family that includes a 32-bit Arm Cortex-M33 core with 76.8 MHz maximum operating frequency plus a 2.4 GHz energy-efficient

radio core with low active and sleep currents and an integrated power amplifier with up to 6-decibel meters (dBm) transmit (TX) power in a $4 \times 4 \times 0.85$ millimeter (mm) QFN32 package (Figure 3). They include secure boot with root of trust and secure loader (RTSL). Additional security features include hardware cryptographic acceleration for AES128/256, SHA-1, SHA-2 (up to 256-bit), ECC (up to 256-bit), ECDSA, and ECDH, and a true random number generator

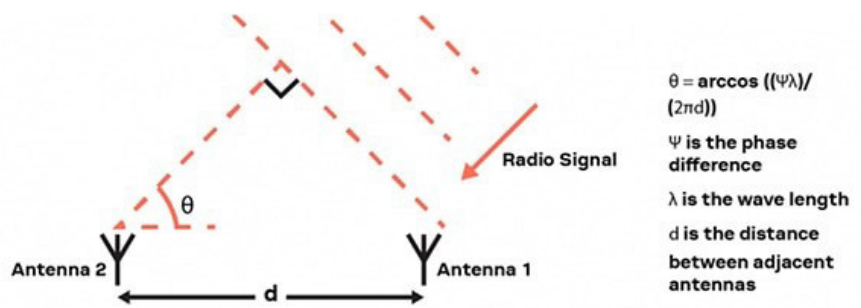


Figure 2: The equation for determining the AoA (top right) uses the phase difference of the arriving signals, the signal wavelength, and the distance between adjacent antennas. *Image source: u-blox*



Figure 3: EFR32BG22 Wireless Gecko Bluetooth SoCs that support AoA and AoD are available in a 4 × 4 × 0.85 mm QFN32 package *Image Source: Silicon Labs*

- Virtual COM port interface provides a serial port connection over Ethernet or USB
- Packet trace interface provides debug information about received and transmitted wireless data packets

(TRNG) compliant with NIST SP800-90 and AIS-31. Additionally, depending on the model, these SoCs have up to 512 kB of flash and 32 kB of RAM, and are available in 5 × 5 × 0.85 mm QFN40, and 4 × 4 × 0.30 mm TQFN32 packages, in addition to a QFN32.

The [BG22-RB4191A](#) wireless pro kit includes a direction-finding radio board based on the 2.4 GHz EFR32BG22 Wireless Gecko SoC and an antenna array optimized for accurate direction finding that can speed development of Bluetooth 5.1-based RTLS applications using AoA and AoD protocols (Figure 4). The mainboard has several tools for easy evaluation and development of wireless applications, including:

- Onboard J-Link debugger for programming and debugging on the target device over Ethernet or USB
- Real-time current and voltage measurements using the advanced energy monitor

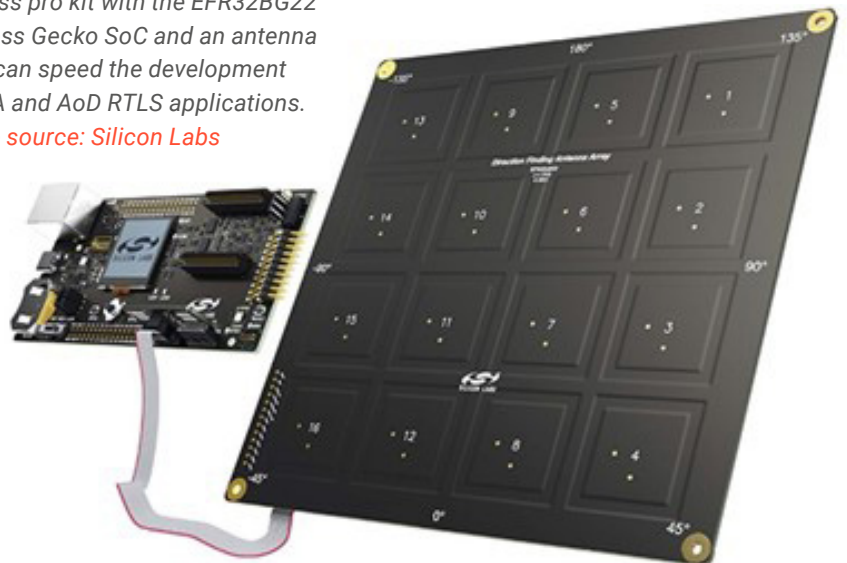
Modules for Bluetooth AoA and AoD

u-blox offers Bluetooth modules with and without integrated antennas that support AoA and AoD. For applications that benefit from a module without an integrated antenna, designers

can turn to the NINA-B41x series, such as the [NINA-B411-01B](#), based on the Nordic Semiconductor [nRF52833](#) IC (Figure 5). These modules include an integrated RF core and Arm Cortex-M4 with a floating point processor and operate in all Bluetooth 5.1 modes, including AoA and AoD. With an operating temperature range from -40 to +105°C, these modules are well suited for RTLS applications in industrial environments. Furthermore, their input voltage range of 1.7 to 3.6 V makes them useful in single-cell battery-powered systems.

The NINA-B40x series from u-blox, such as the [NINA-B406-00B](#), include an internal PCB trace antenna integrated into the 10 x 15 x 2.2 mm module PCB (Figure 6). NINA-B406 modules can deliver up to +8 dBm of output power. In addition to support for Bluetooth

Figure 4: The BG22-RB4191A wireless pro kit with the EFR32BG22 Wireless Gecko SoC and an antenna array can speed the development of AoA and AoD RTLS applications. *Image source: Silicon Labs*



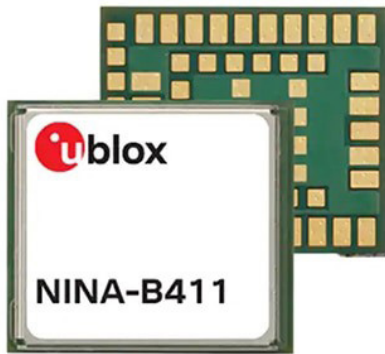


Figure 5: NINA-B41x series modules support compact RTLS solutions that use external antennas

Image source: DigiKey

5.1 modes, including AoA and AoD, these modules support 802.15.4 (Thread and Zigbee) and Nordic proprietary 2.4 GHz protocols, enabling designers to standardize on a single module for a wide range of IoT device designs.

To speed time to market, designers can use the [XPLR-AOA-1](#) explorer kit from u-blox that allows experimentation with the Bluetooth 5.1 direction-finding feature and support for AoA and AoD functions. This explorer kit includes a tag and

Figure 6: AoA and AoD applications that benefit from an integrated antenna can use the NINA-B40x series modules.

Image source: DigiKey



an antenna board with a NINA-B411 Bluetooth LE module (Figure 7). The tag is built around a NINA-B406 Bluetooth module and includes software to send out Bluetooth 5.1 advertisement messages. The antenna board is designed to receive the messages and apply an angle calculation algorithm to determine the direction of the tag. The angles are calculated in two dimensions using the array of antennas on the board.

The flexibility of the XPLR-AOA-1 kit enables designers to explore a variety of applications, such as:

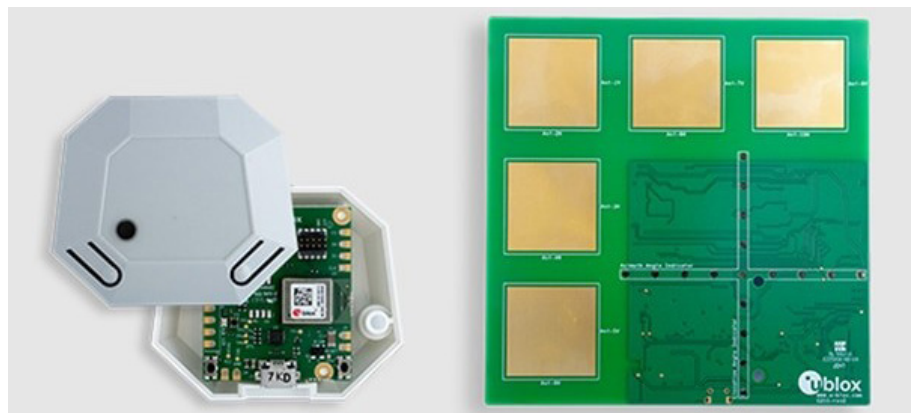
- Detecting if an object is approaching a door
- Enabling a camera to follow an asset moving in a room
- Tracking goods passing through a gate or past a specific position
- Avoiding collisions between robots or automated guided vehicles

In addition, a more complex positioning system can be created using several XPLR-AOA-1 kits and triangulating the directions from three or more antenna boards.

Summary

Bluetooth AoA and AoD can provide accurate and cost-effective RTLS implementations for Industry 4.0. Designers who can select from SoCs and modules that include the software needed to quickly implement the complex software required to deploy Bluetooth AoA and AoD. These SoCs and modules are optimized for low power consumption to support battery-powered location tags and are designed to operate in harsh industrial environments.

Figure 7: The XPLR-AOA-1 explorer kit includes a tag (left) and an antenna board (right) to support evaluation of Bluetooth AoA and AoD. Image source: u-blox



How to select and apply antennas for IoT devices

Written by Steven Keeping

The proliferation of Internet of Things (IoT) devices continues to accelerate and inspire the design of innovative end products. However, designers must remember that no matter how much creativity and effort goes into the hardware and software, the antenna plays a pivotal role. If the antenna does not work right, product performance is severely compromised.

As the interface between the device and the wireless network, the antenna is a critical part of the IoT device design process. It converts electrical energy to an electromagnetic radio-frequency (RF) wave at the transmitter and converts an incoming RF signal to electrical energy at the receiver. Designers can optimize the performance of an application by

selecting an antenna that meets key engineering parameters. However, the many available options and considerations can lead to delayed and costly design cycles.

This article summarizes the role of an antenna in a wireless IoT device and briefly describes the critical design criteria influencing its selection. The article then uses



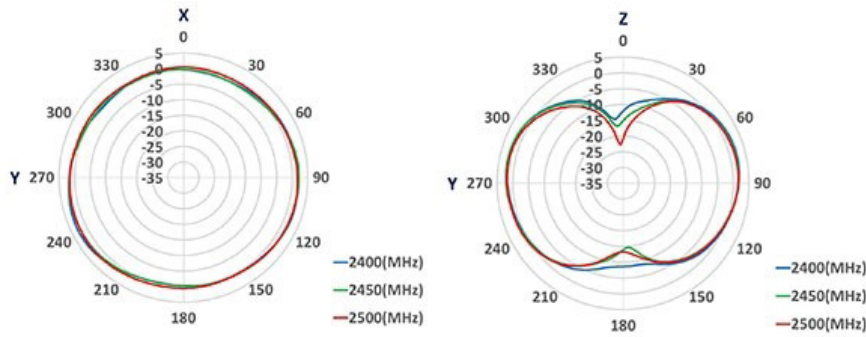


Figure 1: Radiation patterns graphically represent how the antenna radiates or absorbs radio energy in 3D space. Datasheets typically show the maximum extent in the XY and YZ planes when the antenna is mounted as intended.

Image source: Amphenol

example antennas from Amphenol to illustrate suitable choices for a Bluetooth Low Energy (LE) or Wi-Fi sensor, an IoT asset tracker with GNSS satellite positioning capability, a Wi-Fi access point (AP), and a LoRa IoT device.

Interpreting the datasheet

An antenna’s final performance is subject to engineering decisions such as mounting position and the design of impedance matching networks. A good implementation requires a careful review of the antenna’s datasheet. Key parameters include:

- **Radiation pattern:** this graphically defines how the antenna radiates (or absorbs) radio energy in 3D space (Figure 1)
- **Maximum power transfer:** good power transfer between the antenna and receiver occurs when the transmission line impedance (Z_0) is matched to that of the antenna (Z_a).

Poor impedance matching increases return loss (RL). The voltage standing wave ratio (VSWR) indicates the impedance matching between the transmission line and the antenna (Table 1). High VSWR values result in high power losses. A VSWR below 2 is generally acceptable for an IoT product

- **Frequency response:** Return Loss (RL) depends on the radio frequency. Designers should check the datasheet for the antenna’s frequency response to ensure RL is minimized at the intended operating frequency (Figure 2)
- **Directivity:** this measures the directional nature of the antenna’s radiation pattern. Maximum directivity is defined as D_{max}
- **Efficiency (η):** the ratio of total radiated power (TRP, or P_{rad}) to input power (P_{in}) is calculated from the formula $\eta = (P_{rad}/P_{in}) * 100\%$
- **Gain:** this describes how much power is transmitted in the direction of peak radiation. It is usually referenced to an isotropic antenna with a designation of dBi. It is calculated from the formula $Gain_{max} = \eta * D_{max}$

| VSWR | Return Loss (dB) | % Power/Voltage Loss |
|------|------------------|----------------------|
| 1 | - | - |
| 1.25 | -19.1 | 1.2/11.1 |
| 2 | -9.5 | 11.1/33.3 |
| 2.5 | -7.4 | 18.2/42.9 |
| 3.5 | -5.1 | 30.9/55.5 |
| 5 | -3.5 | 44.7/66.6 |
| 10 | -1.7 | 67.6/81.8 |
| 20 | -0.87 | 81.9/90.5 |

Table 1: The VSWR indicates the impedance match between the transmission line and the antenna. A VSWR below 2 is generally acceptable for an IoT product.

Table source: Steven Keeping

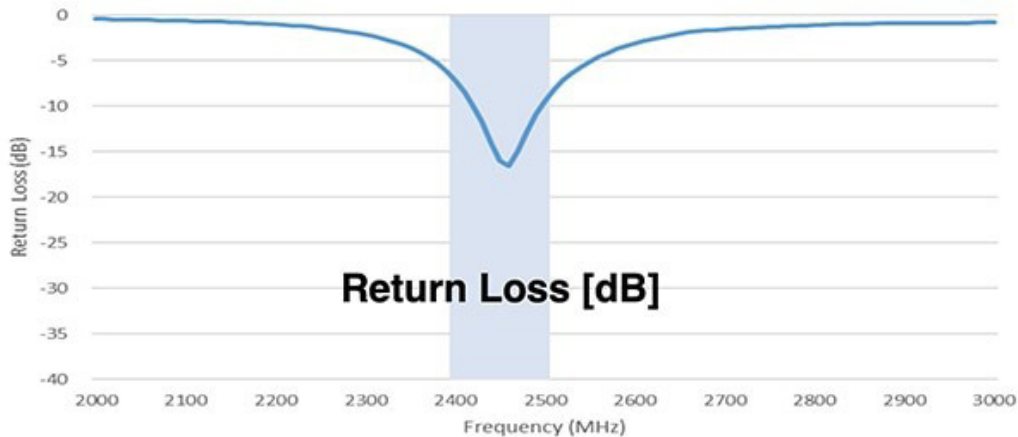


Figure 2: VSWR and RL are dependent on frequency. RL should be minimized at the intended operating frequency. [Image source: Amphenol](#)

Boosting performance

An antenna with poor performance restricts how much electrical power is transformed into radiated energy at the transmitter and how much energy is harvested from incoming RF signals at the receiver. Poor performance at either end reduces the wireless link's range.

The primary factor affecting the antenna's performance is impedance. A significant mismatch between the antenna's impedance (which is related to voltage and current at its input) and the impedance of the voltage source driving the antenna results in poor energy transfer.

A well-designed impedance matching circuit minimizes the VSWR and subsequent power losses by matching the impedance of the transmitter power sources with that of the antenna. The impedance is typically 50 ohms (Ω) for a low-power IoT product.

The antenna's position also

dramatically influences the end product's transmit power and receive sensitivity. For an internal antenna, design guidelines recommend placement at the top of the IoT device on the printed circuit (PC) board edge and as far as possible from other components that could generate electromagnetic interference (EMI) during operation.

Impedance matching components are an exception, as these are proximal to the antenna by necessity. The pc board pads and traces connecting the antenna to the rest of the circuitry should be the only copper conductors in a defined clearance area (Figure 3).

(For more detail on antenna

design guidelines, see "[How to Use Multiband Embedded Antennas to Save Space, Complexity, and Cost in IoT Designs.](#)")

Antenna types

Specifying the antenna is a critical part of the IoT device design process. The antenna should be

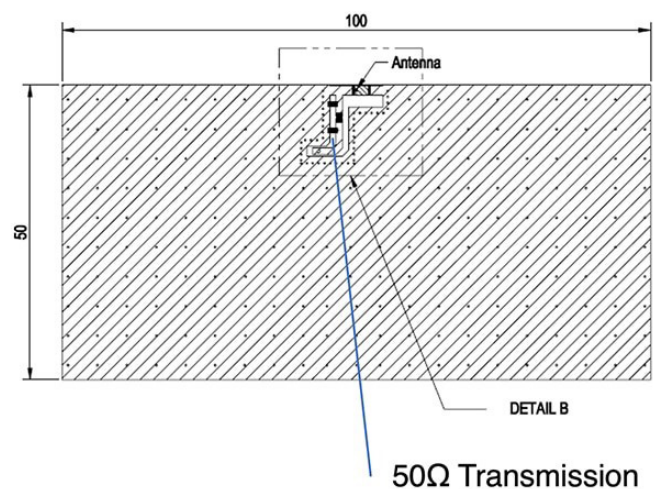


Figure 3: A PC board-mounted antenna should be placed close to the pc board edge. The antenna should also be placed away from other components (apart from those used for the impedance matching circuit) by incorporating a clearance area. [Image source: Amphenol](#)



Figure 4: Different antennas are available to suit various IoT applications. *Image source: Amphenol*

optimized for the target wireless interface's RF band, for example, NB-IoT for multiple bands between 450 megahertz (MHz) and 2200 MHz, LoRa for 902 to 928 MHz in North America, Wi-Fi for 2.4 gigahertz (GHz) and 5 GHz, and Bluetooth LE for 2.4 GHz.

Antennas employ different electrical concepts. Examples are monopole, dipole, loop, inverted F antenna (IFA), and planar inverted-F antenna (PIFA). Each suits a particular application.

There are also single-ended and differential antennas. The single-ended type is unbalanced, while differential antennas are balanced. Single-ended antennas receive or transmit a signal referenced to ground, and the characteristic input impedance is typically 50

Ω . However, because many RF ICs have differential RF ports, a transformation network is often required if a single-ended antenna is employed. This balun network transforms the signal from balanced to *unbalanced*.

A differential antenna transmits using two complementary signals, each in its own conductor. Because the antenna is balanced, no balun is required when the antenna is used with RF ICs with differential RF ports.

Finally, antennas come in several form factors, such as pc board, chip or patch, external whip, and wire. Figure 4 illustrates some sample applications.

Matching the antenna to the application

The application and product form factor determine the final choice of antenna. For example, if an IoT product is space-constrained, a PC board antenna can be incorporated directly into the PC board circuitry. These antennas are an excellent choice for 2.4 GHz applications such as Bluetooth LE or Wi-Fi sensors in smart home devices, including lighting, thermostats, and security systems. They offer reliable RF performance in a low-profile architecture. Still, PC board antennas are tricky to design. An alternative is to source the pc board antenna from a commercial vendor. It can then be attached to the PC board using an adhesive backing.

An example of a PC board

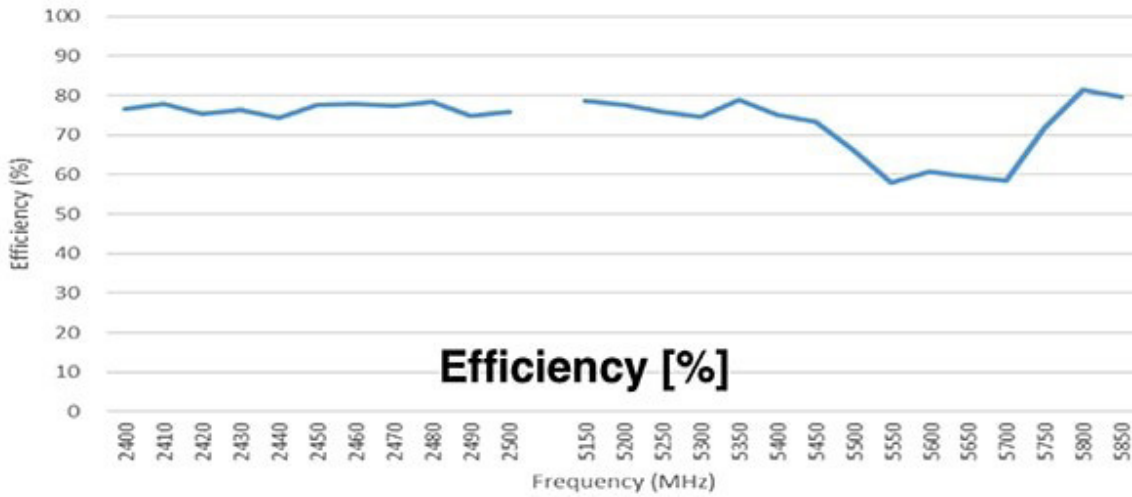


Figure 5: The ST0224-10-401-A Wi-Fi pc board trace antenna is efficient in both the 2.4 and 5 GHz bands. Image source: Amphenol

antenna is Amphenol's [ST0224-10-401-A](#) Wi-Fi PC board trace RF antenna. The antenna offers an omnidirectional radiation pattern in the 2.4 to 2.5 GHz and 5.15 to 5.85 GHz bands. The antenna measures 30 x 10 x 0.2 millimeters (mm) and has an impedance of 50 Ω. Its RL is less than -10 decibels (dB) for both frequency ranges, and its peak gain is 2.1 dBi relative to isotropic (dBi) in the 2.4 GHz band and 3.1 dBi in the 5 GHz band. Its efficiency is 77 and 71%, respectively (Figure 5).

Another option for space-constrained IoT products is a chip antenna. Automated equipment can directly mount this compact component on a PC board. The antenna suits wireless IoT applications based on Bluetooth LE or Wi-Fi. The key advantages of a chip antenna are space savings, reduced manufacturing costs, and a simplified design process.

As described above, the

performance of a chip antenna is influenced by factors such as pc board layout and surrounding components, but advances in antenna technology have resulted in highly efficient devices. Chip antennas suit various applications, from smartphones and tablets to smart home systems and industrial sensors.

An example is Amphenol's [ST0147-00-011-A](#), a 2.4 GHz pc board surface mount chip antenna. The antenna offers an omnidirectional radiation pattern in the 2.4 to 2.5 GHz frequency band (Figure 6). The antenna measures 3.05 x 1.6 x 0.55 mm and has an impedance of 50 Ω. Its RL is less than -7 dB, its peak gain is 3.7 dBi, and its average efficiency is 80%.

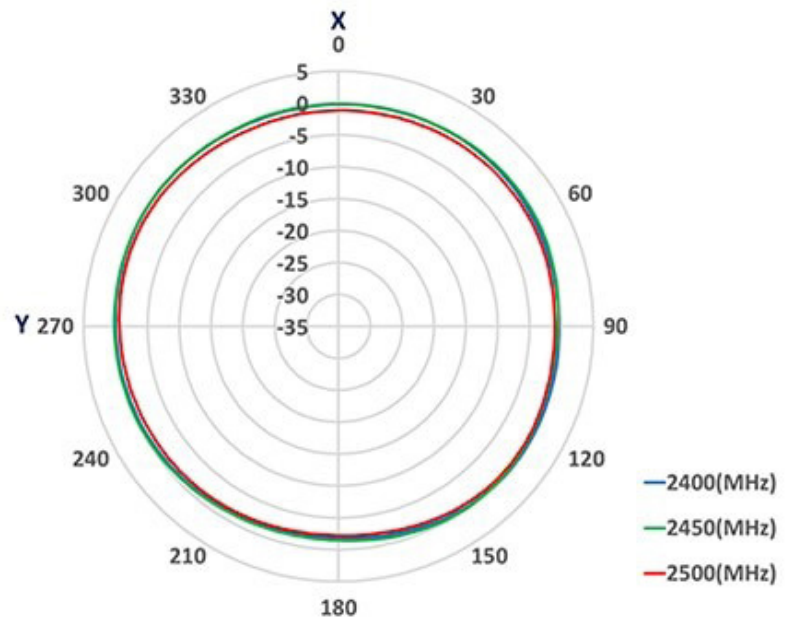


Figure 6: The ST0147-00-011-A surface mount chip antenna is compact and exhibits an omnidirectional radiation pattern in the XY plane. Image source: Amphenol



Figure 7: The ST0226-30-002-A external whip antenna for Wi-Fi APs is available with either an SMA or RP-SMA plug connector. *Image source: Amphenol*

Like PC board antennas, patch antennas are compact and can be directly attached to the PC board. A typical application is an antenna for an asset tracker or other devices with Global Navigation Satellite System (GNSS) capability. GNSS patch antennas comprise a patch element on a dielectric substrate. High efficiency ensures the antenna picks up weak GNSS signals from multiple satellites.



Figure 8: The ST0686-10-N01-U helical wire antenna is a good option for LoRa IoT applications. *Image source: Amphenol*

An example is Amphenol's [ST0543-00-N04-U](#) passive GNSS patch antenna for operation in the 1.575 and 1.602 GHz frequency bands. The antenna measures 18 x 18 x 4 mm and has an impedance of 50 Ω . Its RL is less than -10 dB for both frequency ranges, and its peak gain is -0.5 dBi in the 1.575 GHz band and 1.0 dBi in the 1.602 GHz band. Its efficiency is 80 and 82%, respectively.

External whip antennas, such as the antenna on a Wi-Fi AP, are mounted outside of IoT devices to optimize radio operation. An external whip antenna extends signal range, improves signal quality, and overcomes obstacles or interference. They are useful in environments with weak or obstructed signals, such as those attenuated by walls, ceilings, and furniture in the home. Straight and swivel whip designs, each with standard RF interface connections such as SMA, RP-SMA, and N-Type, are available.

An example is Amphenol's [ST0226-30-002-A](#) 2.4 and 5 GHz SMA RF stick antenna. The antenna is a good solution for Wi-Fi APs and set-top boxes (STBs). It offers an omnidirectional radiation pattern in the 2.4 to 2.5 GHz and 5.15 to 5.85 GHz frequency bands. The antenna measures 88 x 7.9 mm in diameter and has an impedance of 50 Ω . Its RL is less than -10 dB for both frequency ranges, and its peak gain is 3.0 dBi in the 2.4 GHz band and 3.4 dBi in the 5

GHz band. Its efficiency is 86 and 75%, respectively. The antenna is available with either an SMA or RP-SMA plug connector (Figure 7).

Helical wire antennas are an inexpensive and simple option for sub-GHz applications such as LoRa IoT devices operating in the 868 MHz frequency band. The antennas are typically soldered directly to the PC board and offer good performance. Some downsides are bulkiness, particularly when operating at low frequencies, and relatively low efficiency compared with some antenna alternatives.

An example is Amphenol's [ST0686-10-N01-U](#) 862 MHz RF antenna (Figure 8). This helical wire antenna operates in the 862 to 874 MHz frequency band and has an impedance of 50 Ω . The antenna features through-hole solder mounting with a maximum height of 38.8 mm. It has an RL less than -9.5 dB, a peak gain of 2.5 dBi, and an average efficiency of 58%.

Conclusion

Wireless IoT device radio performance depends on antenna selection, so designers must choose carefully from a wide range of antenna designs from suppliers such as Amphenol to best match the application. Datasheets are critical during selection, but following established design guidelines ensures the best wireless performance.



Learn the fundamentals of software-defined radio

Written by Art Pini

From military and aerospace to hobbyists, the promise of software-defined radio (SDR) is that with one piece of hardware, users can capture, demodulate, and access RF signals across a wide swath of radio frequencies. How wide a swath depends upon the hardware's RF front end, while the number and types of signals that can be accessed depends upon the software and underlying processing capabilities. Both of these are a function of the application requirements and the associated cost and power budgets. For military and aerospace, the cost can run into the tens of thousands. For short wave listeners, amateur radio enthusiasts, and do-it-yourselfers (DIYers), what's needed is a simple, low-cost means of accessing radio waves using readily available desktop computers or laptops.

After a brief introduction to SDR, this article introduces a low-cost USB-based SDR module from [Adafruit Industries](#) that can receive and demodulate a wide range of signals, from simple continuous-wave (CW) Morse code to the most complex digital modulation forms. It will show how users can use the module and associated software to add radio reception, radio frequency spectrum, and spectrogram analysis to computers.

What is SDR?

SDR uses digital techniques to replace traditional radio hardware like mixers, modulators, demodulators, and related analog circuits. By digitizing the radio signals directly using an appropriate analog-to-digital converter (ADC), an SDR can

implement all these functions in software so that the same hardware is used for multiple radio modes, whether AM, FM, CW, single sideband (SSB), or double sideband (DSB). The result is an extremely flexible radio that can be quickly reconfigured to handle different signaling technologies (Figure 1).

Traditional radios like the superheterodyne receiver (Figure 1, top) are hardware based and implemented with analog components. The SDR receiver uses an RF tuner to down convert the frequency band of interest to an intermediate frequency (IF) within the range of the ADC. From that point on, all the circuits are digital. The digital down converter translates the signal frequency to baseband, performing a low-pass filtering function. The digital signal processor (DSP) performs demodulation, decoding, and related tasks. These circuits are generally based on application-specific ICs (ASICs), field-programmable gate arrays (FPGAs) and programmable DSP devices. With the appropriate software, these digital circuits provide a very flexible radio capable of receiving a wide range of modulation types.

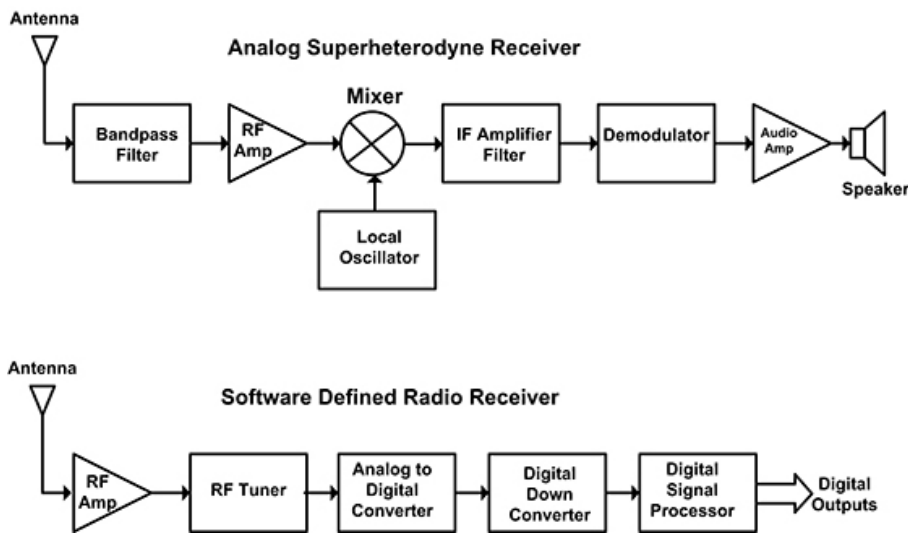


Figure 1: Comparing a traditional analog receiver (top) with an SDR-based receiver (bottom). All functions in the SDR receiver after the ADC are implemented using programmable digital circuits, which allows programmable changes and updates. Image source: Digi-Key Electronics

Low-cost SDR hardware

The Adafruit Industries [1497](#) is a low-cost SDR receiver covering a frequency range of 24 megahertz (MHz) to 1.85 gigahertz (GHz) and is based on a Digital Video

Learn the fundamentals of software-defined radio



Figure 2: The 1497 is a low-cost SDR receiver that fits in a package the size of a quarter and comes with an accessory antenna and remote control. This receiver tunes from 24 MHz to 1.85 GHz, interfacing with a host computer via USB. *Image source: [Adafruit Industries](#)*

Broadcasting – Terrestrial (DVB-T) coded orthogonal frequency-division multiplexing (COFDM) demodulator with a separate tuner IC.

The DVB consortium is a European-based standards organization for the broadcast transmission of digital terrestrial television. This system uses an MPEG transport stream to transmit compressed digital audio, digital video, and other data, using COFDM or OFDM

modulation. These devices can be repurposed by programming to other applications and are ideal for hobbyists and DIYers wanting to listen to and investigate VHF, UHF, and low-microwave-frequency radio signals.

For all the signal processing power in the Adafruit SDR, it has an exceedingly small physical size at only 22.24 millimeters (mm) x 23.1 mm x 9.9 mm (Figure 2). It interfaces with the host computer

via a USB port, and off-the-shelf SDR software provides the user interface on the computer/laptop. The manufacturer recommends Airspy's SDR Sharp (SDR#) in their getting started guide. Software installation takes less than five minutes and is well documented.

The antenna connection on the receiver is through an MCX connector. The MCX jack on the receiver accepts the plug mounted on the antenna cable, or the supplied antenna can be replaced with a user-supplied custom antenna.

If the user decides to replace the supplied antenna with a different one, it can be connected using an MCX plug. Coaxial adaptors can be used to mate the MCX input connector on the SDR with either SMA or BNC connectors, which are more commonly used. [Amphenol RF](#) offers both an MCX plug to SMA jack ([242127](#)) or a BNC jack to MCX

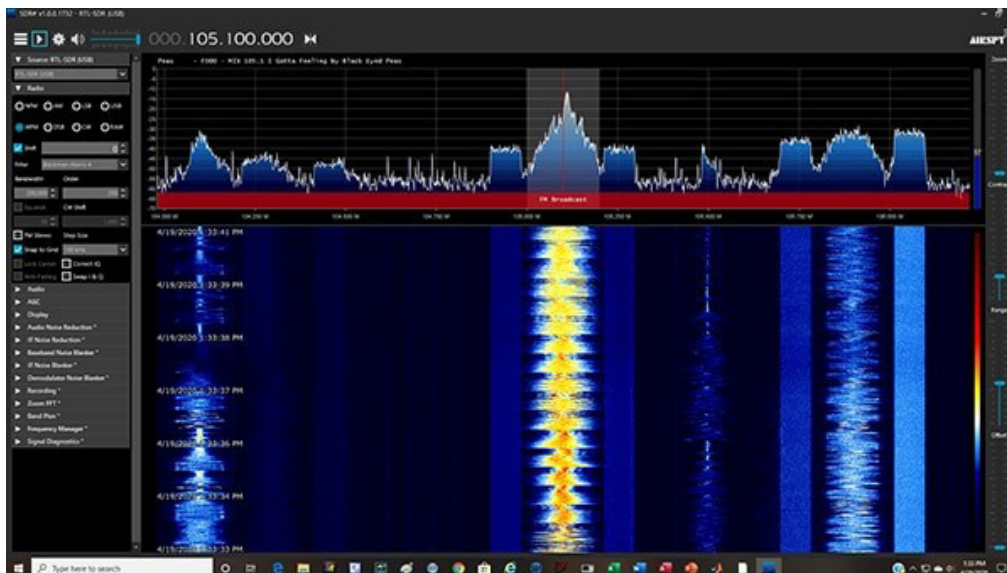


Figure 3: The Airspy SDR# user interface controls the SDR receiver from the drop-down menus on the left. The spectrum analyzer display is shown in the top grid while the spectrum history is below it. *Image source: [Digi-Key Electronics](#)*

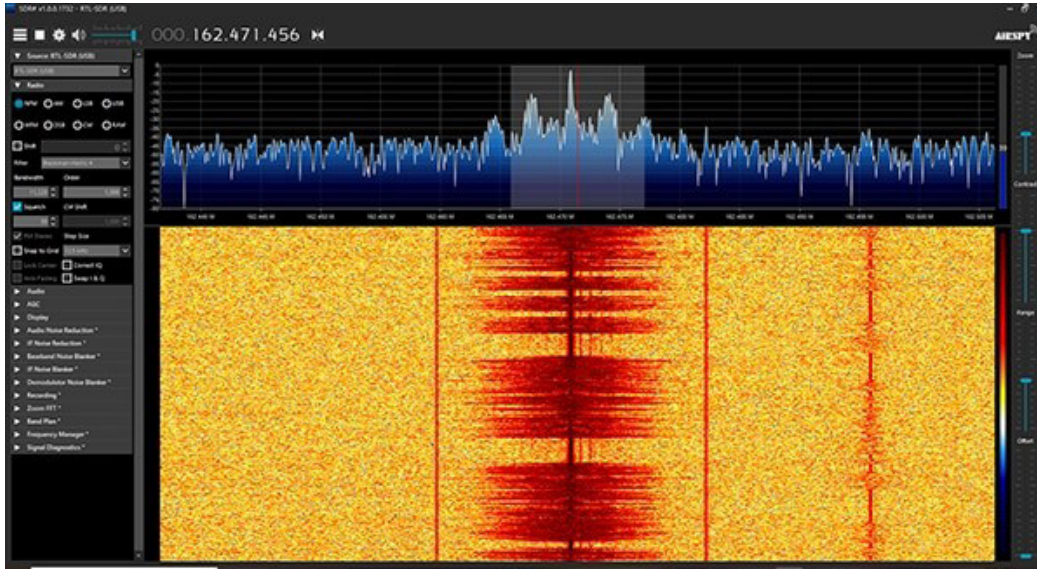


Figure 4: Tuning in a National Weather Service weather broadcast at 162.471 MHz. This station uses narrowband FM. Image source: Digi-Key Electronics

as in the spectrum analyzer display; the vertical scale is time. In the figure there are time markers showing the date and time. The third dimension is the signal power, which is indicated

plug (242204), providing the more common connector interfaces.

SDR support software

The SDR# software connects with the receiver and provides the user interface and visual display (Figure 3).

The SDR# default user interface has three major elements:

- The column on the left contains controls for the SDR device. There are fourteen pull down menus controlling all aspects of the SDR receiver. The principal controls are for the radio, audio, and display
- The top grid contains the spectrum analyzer display. This plots frequency on the horizontal axis and signal power vertically using a logarithmic scale calibrated in decibels. Spectrum analyzers are the primary test tool used by RF engineers to measure and analyze RF devices.

The numeric readout on the top of the screen displays and controls the center frequency of the spectrum analyzer. The maximum displayed frequency range is the bandwidth of the receiver which is about 2 MHz.

There is a horizontal zoom slider control to the right of the display. Zoom permits a horizontal expansion of the display about the center frequency

- Beneath the spectrum analyzer display is a spectrum history display sometimes called a spectrogram, which shows the time history of the spectrum. The horizontal axis is frequency

by the color. The default color scale runs from black, as the minimum power level, to red as the maximum power level. There are a variety of styles and color mappings available under display controls

The signal displayed in Figure 3 is that of an FM broadcast station at 105.1 MHz. This is a wideband FM signal that has a bandwidth of 200 kilohertz (kHz). This is one of eight demodulators available in the SDR receiver. The other demodulators support narrowband FM, AM, upper and lower SSB, DSB, CW, and raw in-phase and quadrature signal components. The selections are in

The antenna connection on the receiver is via an MCX connector. The MCX jack on the receiver accepts a plug mounted on the antenna cable, or the supplied antenna can be replaced with a custom antenna

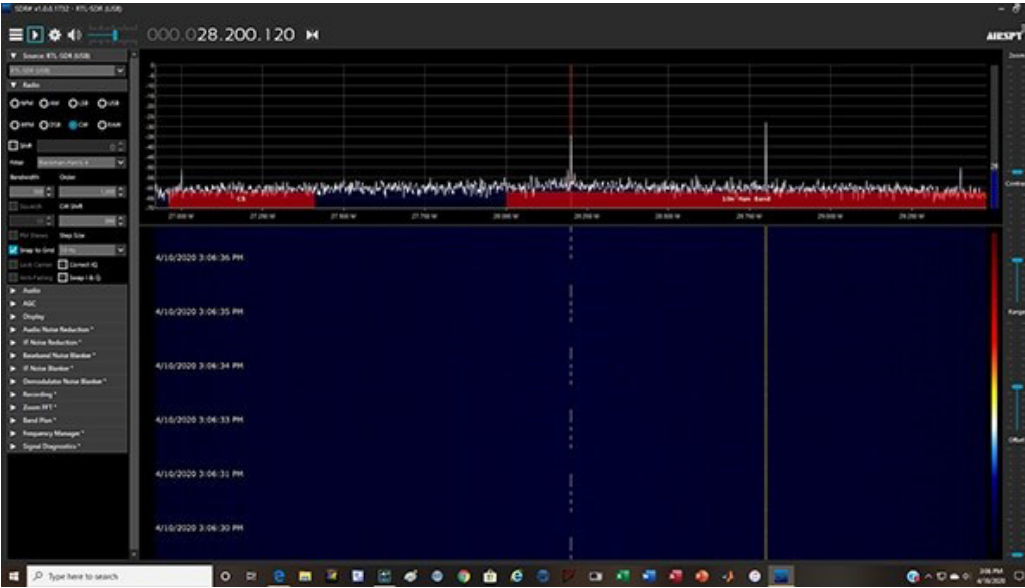


Figure 5: The spectrogram view of a CW Morse code signal. Image source: Digi-Key Electronics

National Weather Service carries only voice and uses narrowband FM (Figure 4).

The National Weather Service station is received using a bandwidth of only 11.2 kHz because the program content is only voice.

the radio controls in the upper left of the display.

The signal spectrum consists of the analog signal about the center frequency. This carries the analog radio program. Outside of that are dual sub-bands that contain other program material and digital information. The program information content is decoded

and appears immediately above the spectrum analyzer display. As well as the spectrum display, the radio station's audio components are available through the host computer for listening.

Wideband FM has a large bandwidth because it is expected to carry high fidelity stereophonic music. A radio service such as the

Again, the audio program material is available as well as the spectrum displays. The SDR receiver adds all of these services to the host computer.

The spectrum history or spectrogram display is useful for seeing changes in the received signals spectrum over time. A

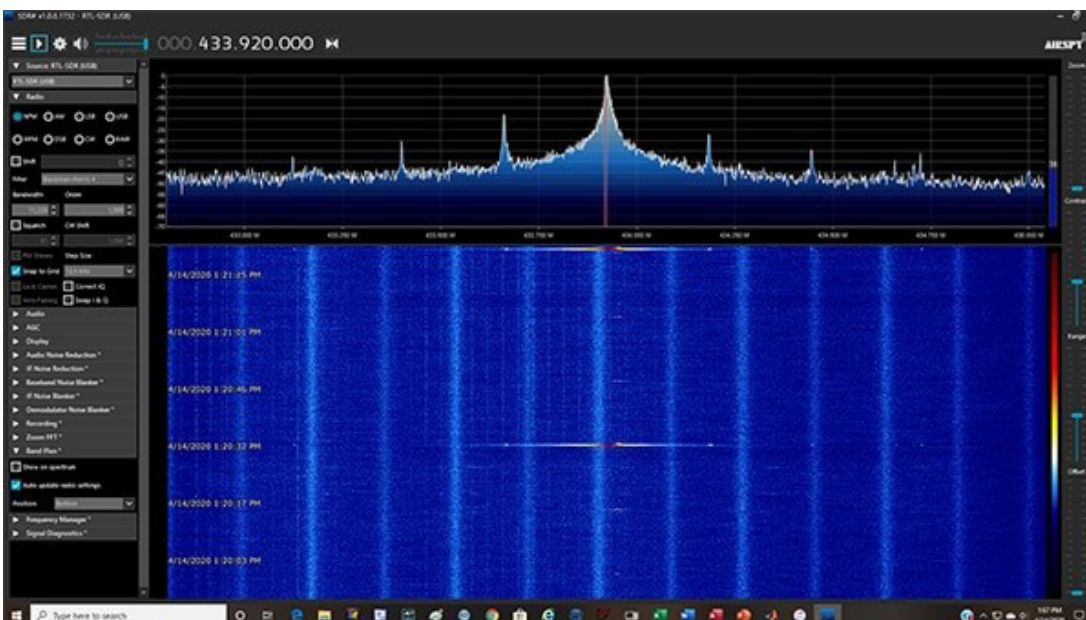
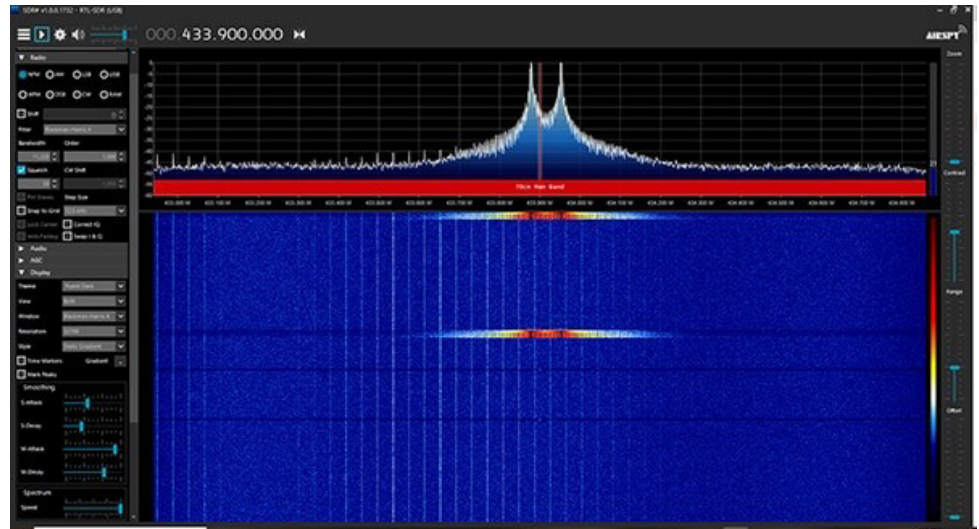


Figure 6: The spectrogram of a remote weather station transmitter at 433.92 MHz that sends data in bursts. The spectrogram captures and displays transmitted bursts roughly 50 seconds apart. Image source: Digi-Key Electronics

Figure 7: The spectrum of a remote keyless entry device uses FSK of a 433.9 MHz carrier to encode digital data to control entry into a vehicle.

Image source: [Digi-Key Electronics](#)



simple example is to see that of a continuous wave (CW) Morse code signal (Figure 5).

CW signals encode data by turning an RF carrier on and off (on-off keying). On the spectrogram display the periods when the key is down – and the carrier is being transmitted – are indicated by the light blue-grey track on the display. The Morse character “V” (di di di dah) indicating testing can be seen in the signal track. Note that the software makes provision for receiving CW signals by supplying a beat frequency oscillator (BFO) labelled “CW shift” to provide a user-controlled audio tone to hear the code transmission. Since CW transmissions are narrowband, the receiver reduces the bandwidth to 300 hertz (Hz) as seen in the radio control pull-down menu. Keeping the receiver bandwidth to the minimum value needed for the mode being received minimizes the noise level in the channel.

Some measurement applications for an SDR receiver

In an increasingly linked world, there are many RF sources that need to be checked and serviced. An example is the verification of the update period of a remote weather station transmitter module (Figure 6).

The spectrogram shows two RF bursts at the remote transmitter’s 433.93 MHz carrier frequency. The time scale on the spectrogram indicates that the FM bursts occur roughly 50 seconds apart.

Automotive remote keyless entry (RKE) systems operate at either at 315 or 433 MHz, depending on where the vehicle is being used and the governing regulations. In this case, the user just needs to hold the key fob near the antenna and push one of the buttons to see the type of modulation used (Figure 7).

The spectrum of the RKE key fob

shows dual peaks at about 433.9 MHz. Data encoding for this device uses frequency shift keying (FSK) where the carrier is shifted between two frequencies to indicate a digital one or zero. Other RKE fobs use amplitude shift keying (ASK) where the amplitude of a carrier is shifted between two levels, not too different from the CW signal.

Conclusion

The Adafruit 1497 SDR receiver opens up the whole world of VHF, UHF, and low microwave frequency bands to investigation hobbyists and professionals alike. It enables users to use a computer to tune into FM, TV, amateur radio, citizens band, weather, and short-wave broadcasts. It also can be used as a spectrum analyzer to verify the operation of a wide range of portable RF devices. The 1497 has also been used to create interferometers for radio astronomy – all at low cost.

The parts we sell help lives become richer

Imagine hearing aids that let a child experience her parents' voice clearly for the first time.

At DigiKey, the parts we sell help companies turn innovative, game-changing ideas into real-world solutions that change lives.

Find your part at [digikey.com](https://www.digikey.com)



DigiKey

we get technical

DigiKey is an authorized distributor for all supplier partners. New products added daily. DigiKey and DigiKey Electronics are registered trademarks of DigiKey Electronics in the U.S. and other countries. © 2025 DigiKey Electronics, 701 Brooks Ave. South, Thief River Falls, MN 56701, USA

 **ECIA MEMBER**
Supporting The Authorized Channel